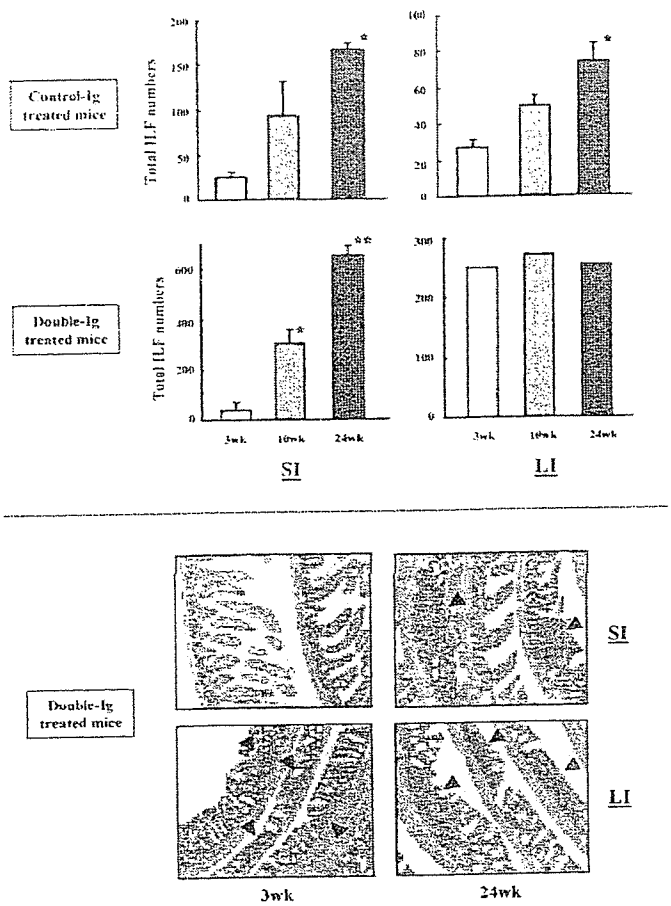

FIGURE 4. Chronological influences on the increased LI-ILF development in mice in utero treated with LTβR-Ig and TNFR55-Ig (double Ig). Numbers of ILF in the small and large intestines (SI and LI, respectively) of mice treated in utero with control Ig or double Ig fusion protein under the stereomicroscopy, as described in Fig. 1 legend. For the H&E staining, the sections were viewed under ×20 optics with a digital light microscope. The progenies were sacrificed, and the total number of ILF in a whole small and large intestine at 3, 10, and 24 wk old was counted. The results are expressed the mean ± SE from three mice per group and from a total of two experiments. *, $p < 0.05$, and **, $p < 0.01$ when compared with the number of ILF of the 3-wk-old progeny.

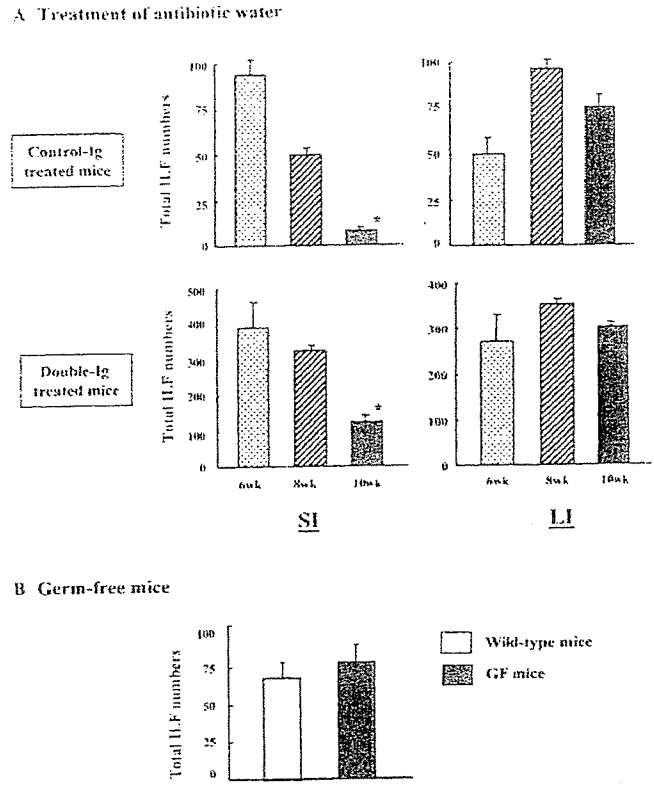

FIGURE 5. Effects of gut microflora on the formation and development of ILF in the small and large intestine. *A*, Both groups of 6-wk-old mice treated with control or LTβR-Ig and TNFR55-Ig (double Ig) fusion protein in utero were fed for 4 wk with antibiotic water containing ampicillin, neomycin sulfate, and streptomycin. At 2 wk (8 wk old) or 4 wk (10 wk old) after antibiotic treatment, the total number of ILF in a whole small and large intestine was counted under light microscope, as described in the Fig. 1 legend. *B*, The total number of ILF in the large intestine of germfree mice was counted. The results are expressed as the mean ± SE from three mice per group and from a total of three experiments. *, $p < 0.05$ when compared with non-antibiotic-treated mice.

The development of LI-ILF is independent from influences of gut microflora

Several previous studies have demonstrated a critical role of gut microflora on the ILF formation in the small intestine (8, 20, 29). To determine the potential involvement of intestinal microflora on the ILF hyperplasia in the large intestine following the prenatal blockage of LTβR and TNFR55 signals, we altered the microflora by oral administration of antibiotic water, which reduced both aerobic and anaerobic bacteria (29). Both groups of 6-wk-old progenies were fed antibiotic water for 4 wk and sacrificed at 2 and 4 wk after feeding. To see the effectiveness of the antibiotic treatment, the bacteria load was determined in the feces of control Ig- and double Ig-treated mice before and after antibiotic treatment. Essentially, no bacteria were remaining after the feeding of antibiotic water (data not shown). As shown in Fig. 5*A*, the antibiotic water treatment drastically decreased ILF formation in the small intestine in both groups of mice treated in utero with control Ig or double Ig. However, strikingly, LI-ILF formation in the double Ig-treated progeny was not influenced by the antibiotic treatment. and maximum numbers of LI-ILF were not changed even after prolonged antibiotic water treatment (Fig. 5*A*). Furthermore, the numbers of LI-ILF were comparable in the germfree mice to those of wild-type mice (Fig. 5*B*). These results indicate that development of ILF in the large intestine is not influenced by the gut bacterial flora.

LI-ILF possess M cells on the FAE region and express AID mRNA

To determine whether LI-ILF possess the ability of Ag uptake from the lumen of intestine, we examined the presence of M cells on the FAE of LI-ILF from the double Ig-treated mice. As indicated in Fig. 6*A*, LI-ILF revealed a hallmark feature of M cells, i.e., a depressed surface with short and irregular microvilli. These results suggest that LI-ILF might play as Ag sampling site as like as the other organized mucosa-associated lymphoid tissues, e.g., colonic patches.

To assess the ability of IgA class switching in the LI-ILF, the expression levels of AID mRNA, which plays an essential role in class switching recombination and somatic hypermutation of Ig genes, were determined (32). The mononuclear cells isolated from LI-ILF of mice treated with double Ig in utero expressed AID mRNA (Fig. 6*B*). In contrast to ILF, AID mRNA was not detectable in the diffused LP region of the large intestine (Fig. 6*B*). These findings suggest that the levels of μ to α class switching are increased in the large intestine of mice treated with double Ig in utero due to the maximum increase of ILF numbers. Thus, one can

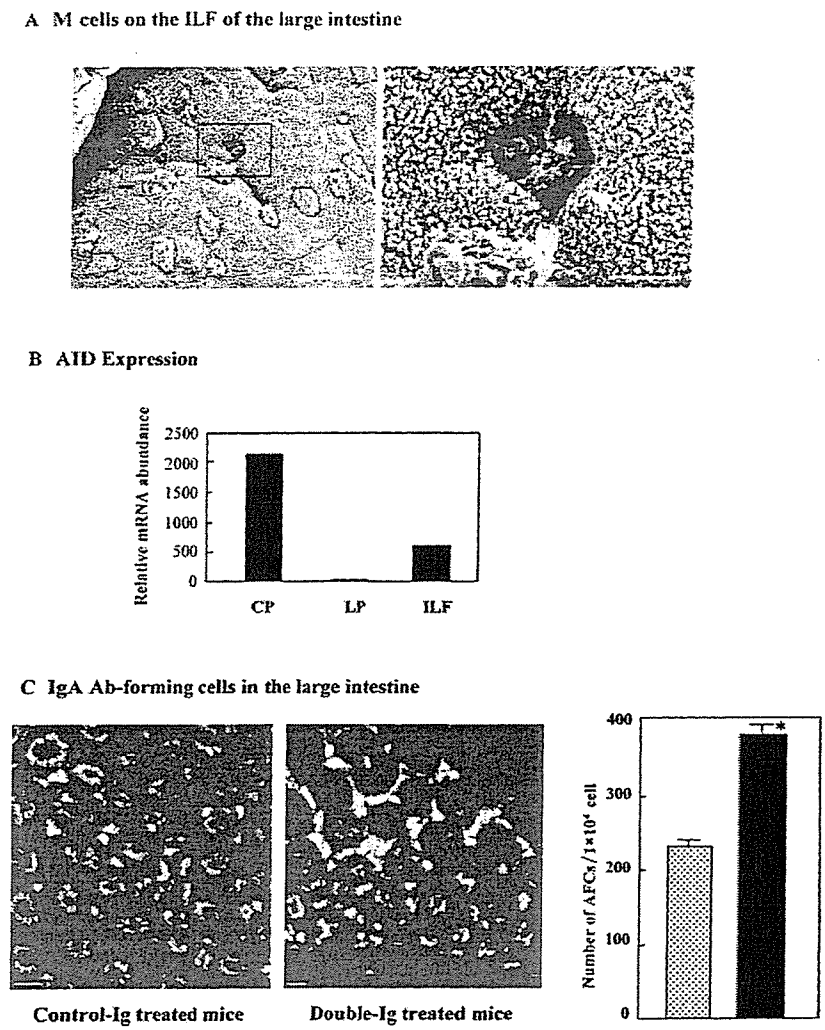

FIGURE 6. *A*, The presence of M cells on the FAE of LI-ILF of mice prenatally treated with LTβR-Ig and TNFR55-Ig (double Ig) fusion protein. *B* and *C*, The mRNA expression of AID and the number of IgA Ab-secreting cells in the large intestine of mice treated with control Ig or double Ig fusion protein in utero. A quantitative RT-PCR was performed using mononuclear cells isolated from LP in the large intestine of control Ig-treated mice and from ILF in the large intestine of double Ig-treated mice. As positive control for a quantitative RT-PCR, CP of control Ig-treated mice were adopted. For the immunohistochemical study (*C, left*), the large intestine of 6-wk-old progenies of both groups were rapidly frozen, and cryostat sections were stained with FITC-conjugated anti-IgA. ELISPOT assay was adopted to further confirm the number of IgA Ab-forming cells in the LP of the large intestine of mice treated with control Ig (▨) or double Ig (■) fusion protein in utero (*C, right*). The results are expressed as the mean ± SE from five mice per group and from a total of two experiments. The bar indicates 10 μm (*A, left*) and 2.5 μm (*A, right*).

predict the subsequent elevation of IgA-producing cells in the large intestine of these mice. The numbers of IgA-producing cells were therefore assessed, using the large intestine of the 6-wk-old mice treated in utero with control Ig or double Ig. Interestingly, increased numbers of IgA-expressing cells were detected in the LP region of the large intestine of in utero double Ig-treated mice when compared with the control mice (Fig. 6*C, left*). The results were also confirmed by the analysis of single cells using ELISPOT assay. The numbers of IgA-producing cells were increased in mononuclear cells isolated from the large intestine of mice treated with double Ig in utero when compared with the control Ig-treated mice (Fig. 6*C, right*). These results further support a notion that ILF may play a role for induction of IgA^+ B cells in the large intestine.

Discussion

In general, a family of inflammatory cytokine-mediated signals provided via LTβR and TNFR55 is considered to be critical for the organogenesis of secondary lymphoid tissue (18, 33). One can consider the organogenic steps that take place during development as a form of programmed inflammation, given what we now know about the steps underlying the genesis of tertiary lymphoid structures in chronic disease settings (34). In this study, we demonstrated that prenatal blockage of LT/LTβR signaling cascade resulted in the acceleration of ILF formation in the large intestine, and further that prenatal blockage of TNF/TNFR55 signal enhanced their maturation. The hyperplasia of LI-ILF was not due to stimulation of exogenous environmental stimuli, such as microflora Ags. Most interestingly, LI-ILF expressed AID mRNA, and therefore might be critically involved in the generation of IgA-committed B cells. Thus, our present study is the first one to show the unique characteristics of LI-ILF as IgA-inductive sites, whose development is accelerated by the blockage of LTβR and TNFR55 in utero.

Normal numbers of ILF were present in the small intestine of mice treated with LTβR-Ig fusion protein in utero, but were absent in the $LT\alpha^{-/-}$ mice and $aly/aly^{-/-}$ mice, suggesting that ILF formation in the small intestine did not require gestational LT/LTβR-dependent event, but needed the postnatal signals (8). In addition, a recent study demonstrated that, unlike PP, postnatal LT/LTβR signals are required for ILF formation in the small intestine, and additional TNF/TNFR55 signal and exogenous stimuli were needed for their maturation (20). In contrast, limited information is currently available on the immunological function and tissue genesis of ILF (or solitary lymphoid aggregates) in the large intestine. For example, in utero treatment with LTβR-Ig ablated the formation of CP, but scattered B cell aggregates in the mucosal layer of large intestine were retained (23). Furthermore, the progeny of mice treated with LTβR-Ig plus TNFR55-Ig fusion protein were reported to have some submucosal lymphoid patches in the large intestine (24). In the present study, we demonstrate that prenatal blockage of LT/LTβR signal enhanced the formation of LI-ILF,

and prenatal blockage of LT/LTβR plus TNF/TNFR signals further accelerated this phenomenon and resulted in extreme hyperplasia of LI-ILF. It is clear that LI-ILF used LT/LTβR and TNF/TNFR signals in a different manner than other gut-associated lymphoid tissues such as PP and CP. An interesting possibility is that LTβR- and TNFR-mediated signaling might behave as a negative regulation for the LI-ILF genesis in the gestational period.

Several recent studies demonstrated a critical involvement of gut flora on the development of ILF in the small intestine. It has been reported that normal numbers of ILF were detected in the small intestine of germfree mice (8). However, another study showed that the development of ILF in the small intestine did not occur in germfree mice, but, if germfree mice were conventionalized, modest number of mature ILF developed (20). Further augmentation of ILF formation in the small intestine was induced by in utero treatment with LTβR-Ig fusion protein (20). Fagarasan et al. (29) recently revealed that alteration of bacteria flora by antibiotic treatment abolished ILF hyperplasia and germinal center enlargement in the small intestine that was provoked by the genetic deficiency of AID. Furthermore, the number of anaerobic bacteria was 100-fold increased in the small intestines of $AID^{-/-}$ mice than $AID^{+/-}$; however, no significant changes were detected in the large intestine of $AID^{-/-}$ mice (29). Those results are consistent with our present results showing that the total number of ILF in the small intestine of naive mice and mice treated with double Ig in utero was significantly reduced by antibiotic treatment. However, the formation of LI-ILF of both naive and the double Ig-treated mice was not influenced by the antibiotic treatment. The fact that extreme hyperplasia of ILF in the large intestine of double Ig-treated mice was not due to stimulation of gut microflora suggests that bacterial Ag may not be involved in the development and maturation of LI-ILF. Hence, although the immunological nature of ILF in the small and large intestine seems identical in terms of cell populations and morphologic features, regulatory factors associated with programmed inflammation for their tissue genesis and maturation might be significantly different due to the different exogenous environments. We are investigating the exact regulatory factors that are specifically involved in the development of LI-ILF. In particular, an understanding of the identification and ontogeny of the cells required to induce local LI-ILF formation will be critical, as it appears these cells require LTβR and TNFR signals during embryogenesis that regulate their activity. Furthermore, the identity and regulation of the specific molecules critical for induction of LI-ILF need further study, as it is likely that these are further involved in the regulation of colon-associated diseases.

We have also demonstrated that ILF are abundantly developed in the large intestine in the absence of CP. These plentiful ILF that developed in CP-null large intestine could be a key site for the continuous generation of IgA-committed B cells. Interestingly, our present study showed mononuclear cells isolated from CP and ILF of normal mice, but not from intestinal LP, expressed high levels of AID mRNA that play an essential role for isotype switching recombination and somatic hypermutation of Ig. Furthermore, enhanced numbers of IgA-producing cells were noted in the LP region of large intestine of progenies with numerous numbers of ILF, but no CP by the gestational blockage of LT/LTβR and TNF/TNFR55 signaling pathways. Based upon their cell phenotype and micro- and macromorphology, it is reasonable to classify LI-ILF as an inductive site for intestinal IgA production in addition to CP. Therefore, LI-ILF and CP may form a reciprocal inductive network in mucosal immunity. Thus, the increased IgA response seen in the CP-null mice could be explained as a compensatory response in the absence of CP. Taken together, both ILF and CP in the large intestine are integrated inductive tissues that can compensate each other for the induction of mucosal IgA responses.

A possible contribution of LI-ILF to the development of colon-restricted inflammatory disease is just beginning to be understood. A previous study described that elimination of PP and CP, but not scattered aggregates of B cells by in utero treatment with LTβR-Ig fusion protein, resulted in the prevention of trinitrobenzenesulfonic acid-induced Th2 cell type colitis development (23). In contrast, another group found a more severe type of dextran sodium sulfate-induced colitis in PP- and mesenteric lymph node-null mice generated by the in utero treatment with LTβR-Ig and TNFR55-Ig fusion proteins (24). Although these mice did not possess peripheral lymphoid tissue, they found that there were submucosally located lymphoid follicles in the large intestine consisting of B and T cell areas. Furthermore, dextran sodium sulfate-induced colitis accelerated additional formation of these lymphoid follicles (24). In all cases of ulcerative colitis patients, the colonic LP contain numerous basal lymphoid aggregates composed of T and B lymphocytes and dendritic cells (35). Furthermore, these lymphoid aggregates increase in number and size with severity of disease (35). Overall, it seems likely that LI-ILF could be site for the generation of regulatory and/or pathogenic lymphocytes. Thus, both in human patients and in mouse disease models, LI-ILF hyperplasia is associated with colonic disease. Furthermore, whether ILF induces regulatory type responses or pathogenic type responses may depend on surrounding environmental and immunological conditions. To further address these questions, our murine model of LI-ILF hyperplasia will be useful to clarify their precise role in the control of large intestine-restricted diseases.

Disclosures

The authors have no financial conflict of interest.

References

1. Kiyono, H., J. Bienenstock, J. R. McGhee, and P. B. Ernst. 1992. The mucosal immune system: features of inductive and effector sites to consider in mucosal immunization and vaccine development. *Reg. Immunol. 4:54.*
2. McGhee, J. R., and H. Kiyono. 1999. The mucosal immune system. In *Fundamental Immunology*, 4th Ed. W. E. Paul, ed. Lippincott-Raven Publishers, New York, p. 909.
3. Keren, D. F., P. S. Holt, H. H. Collins, P. Gemski, and S. B. Formal. 1978. The role of Peyer's patches in the local immune response of rabbit ileum to live bacteria. *J. Immunol. 120:1892.*
4. Craig, S. W., and J. J. Cebra. 1971. Peyer's patches: an enriched source of precursors for IgA-producing immunocytes in the rabbit. *J. Exp. Med. 134:188.*
5. Yamamoto, M., P. Rennert, J. R. McGhee, M. N. Kweon, S. Yamamoto, T. Dohi, S. Otake, H. Bluethmann, K. Fujihashi, and H. Kiyono. 2000. Alternate mucosal immune system: organized Peyer's patches are not required for IgA responses in the gastrointestinal tract. *J. Immunol. 164:5184.*
6. Kang, H. S., R. K. Chin, Y. Wang, P. Yu, J. Wang, K. A. Newell, and Y. X. Fu. 2002. Signaling via LTβR on the lamina propria stromal cells of the gut is required for IgA production. *Nat. Immunol. 3:576.*
7. Fagarasan, S., K. Kinoshita, M. Muramatsu, K. Ikuta, and T. Honjo. 2001. In situ class switching and differentiation to IgA-producing cells in the gut lamina propria. *Nature 413:639.*
8. Hamada, H., T. Hiroi, Y. Nishiyama, H. Takahashi, Y. Masunaga, S. Hachimura, S. Kaminogawa, H. Takahashi-Iwanaga, T. Iwanaga, H. Kiyono, et al. 2002. Identification of multiple isolated lymphoid follicles on the antimesenteric wall of the mouse small intestine. *J. Immunol. 168:57.*
9. Smith, C. A., T. Farrah, and R. G. Goodwin. 1994. The TNF receptor superfamily of cellular and viral proteins: activation, costimulation, and death. *Cell 76:959.*
10. Ware, C. F., T. L. VanArsdale, P. D. Crowe, and J. L. Browning. 1995. The ligands and receptors of the lymphotoxin system. *Curr. Top. Microbiol. Immunol. 198:175.*
11. Vandenabeele, P., W. Declercq, B. Vanhaesebroeck, J. Grooten, and W. Fiers. 1995. Both TNF receptors are required for TNF-mediated induction of apoptosis in PC60 cells. *J. Immunol. 154:2904.*
12. Gruss, H. J., and S. K. Dower. 1995. Tumor necrosis factor ligand superfamily: involvement in the pathology of malignant lymphomas. *Blood 85:3378.*
13. Browning, J. L., I. D. Sizing, P. Lawton, P. R. Bourdon, P. D. Rennert, G. R. Majeau, C. M. Ambrose, C. Hession, K. Miatkowski, D. A. Griffiths, et al. 1997. Characterization of lymphotoxin-$\alpha\beta$ complexes on the surface of mouse lymphocytes. *J. Immunol. 159:3288.*
14. De Togni, P., J. Goellner, N. H. Ruddle, P. R. Streeter, A. Fick, S. Mariathasan, S. C. Smith, R. Carlson, L. P. Shornick, and J. Strauss-Schoenberger. 1994.

Abnormal development of peripheral lymphoid organs in mice deficient in lymphotoxin. *Science 264:703.*

15. Alimzhanov, M. B., D. V. Kuprash, M. H. Kosco-Vilbois, A. Luz, R. L. Turetskaya, A. Tarakhovsky, K. Rajewsky, S. A. Nedospasov, and K. Pfeffer. 1997. Abnormal development of secondary lymphoid tissues in lymphotoxin β-deficient mice. *Proc. Natl. Acad. Sci. USA 94:9302.*
16. Futterer, A., K. Mink, A. Luz, M. H. Kosco-Vilbois, and K. Pfeffer. 1998. The lymphotoxin β receptor controls organogenesis and affinity maturation in peripheral lymphoid tissues. *Immunity 9:59.*
17. Koni, P. A., R. Sacca, P. Lawton, J. L. Browning, N. H. Ruddle, and R. A. Flavell. 1997. Distinct roles in lymphoid organogenesis for lymphotoxins α and β revealed in lymphotoxin β-deficient mice. *Immunity 6:491.*
18. Rennert, P. D., J. L. Browning, and P. S. Hochman. 1997. Selective disruption of lymphotoxin ligands reveals a novel set of mucosal lymph nodes and unique effects on lymph node cellular organization. *Int. Immunol. 9:1627.*
19. Rennert, P. D., J. L. Browning, R. Mebius, F. Mackay, and P. S. Hochman. 1996. Surface lymphotoxin α/β complex is required for the development of peripheral lymphoid organs. *J. Exp. Med. 184:1999.*
20. Lorenz, R. G., D. D. Chaplin, K. G. McDonald, J. S. McDonough, and R. D. Newberry. 2003. Isolated lymphoid follicle formation is inducible and dependent upon lymphotoxin-sufficient B lymphocytes, lymphotoxin β receptor, and TNF receptor I function. *J. Immunol. 170:5475.*
21. Owen, R. L., A. J. Piazza, and T. H. Ermak. 1991. Ultrastructural and cytoarchitectural features of lymphoreticular organs in the colon and rectum of adult BALB/c mice. *Am. J. Anat. 190:10.*
22. Dohi, T., K. Fujihashi, P. D. Rennert, K. Iwatani, H. Kiyono, and J. R. McGhee. 1999. Hapten-induced colitis is associated with colonic patch hypertrophy and T helper cell 2-type responses. *J. Exp. Med. 189:1169.*
23. Dohi, T., P. D. Rennert, K. Fujihashi, H. Kiyono, Y. Shirai, Y. I. Kawamura, J. L. Browning, and J. R. McGhee. 2001. Elimination of colonic patches with lymphotoxin β receptor-Ig prevents Th2 cell-type colitis. *J. Immunol. 167:2781.*
24. Spahn, T. W., H. Herbst, P. D. Rennert, N. Lugering, C. Maaser, M. Kraft, A. Fontana, H. L. Weiner, W. Domschke, and T. Kucharzik. 2002. Induction of colitis in mice deficient of Peyer's patches and mesenteric lymph nodes is associated with increased disease severity and formation of colonic lymphoid patches. *Am. J. Pathol. 161:2273.*
25. Eugster, H. P., M. Muller, U. Karrer, B. D. Car, B. Schnyder, V. M. Eng, G. Woerly, M. Le Hir, F. di Padova, M. Aguet, et al. 1996. Multiple immune abnormalities in tumor necrosis factor and lymphotoxin-α double-deficient mice. *Int. Immunol. 8:23.*
26. Force, W. R., B. N. Walter, C. Hession, R. Tizard, C. A. Kozak, J. L. Browning, and C. F. Ware. 1995. Mouse lymphotoxin-β receptor: molecular genetics, ligand binding, and expression. *J. Immunol. 155:5280.*
27. Miller, G. T., P. S. Hochman, W. Meier, R. Tizard, S. A. Bixler, M. D. Rosa, and B. P. Wallner. 1993. Specific interaction of lymphocyte function-associated antigen 3 with CD2 can inhibit T cell responses. *J. Exp. Med. 178:211.*
28. Kweon, M. N., M. Yamamoto, M. Kajiki, I. Takahashi, and H. Kiyono. 2000. Systemically derived large intestinal $CD4^+$ Th2 cells play a central role in STAT6-mediated allergic diarrhea. *J. Clin. Invest. 106:199.*
29. Fagarasan, S., M. Muramatsu, K. Suzuki, H. Nagaoka, H. Hiai, and T. Honjo. 2002. Critical roles of activation-induced cytidine deaminase in the homeostasis of gut flora. *Science 298:1424.*
30. Bunda, S., N. Kaviani, and A. Hinek. 2005. Fluctuations of intracellular iron modulate elastin production. *J. Biol. Chem. 280:2341.*
31. Fujihashi, K., J. R. McGhee, M. N. Kweon, M. D. Cooper, S. Tonegawa, I. Takahashi, T. Hiroi, J. Mestecky, and H. Kiyono. 1996. γ/δ T cell-deficient mice have impaired mucosal immunoglobulin A responses. *J. Exp. Med. 183:1929.*
32. Muramatsu, M., K. Kinoshita, S. Fagarasan, S. Yamada, Y. Shinkai, and T. Honjo. 2000. Class switch recombination and hypermutation require activation-induced cytidine deaminase (AID), a potential RNA editing enzyme. *Cell 102:553.*
33. Rennert, P. D., D. James, F. Mackay, J. L. Browning, and P. S. Hochman. 1998. Lymph node genesis is induced by signaling through the lymphotoxin β receptor. *Immunity 9:71.*
34. Kratz, A., A. Campos-Neto, M. Hanson, and N. Ruddle. 1996. Chronic inflammation caused by lymphotoxin is lymphoid neogenesis. *J. Exp. Med. 183:1461.*
35. Yeung, M. M., S. Melgar, V. Baranov, A. Oberg, A. Danielsson, S. Hammarstrom, and M. L. Hammarstrom. 2000. Characterization of mucosal lymphoid aggregates in ulcerative colitis: immune cell phenotype and TcR-γδ expression. *Gut 47:215.*

Intestinal γδ T Cells Develop in Mice Lacking Thymus, All Lymph Nodes, Peyer's Patches, and Isolated Lymphoid Follicles[1]

Satoshi Nonaka,* Tomoaki Naito,* Hao Chen,* Masafumi Yamamoto,‡ Kazuyo Moro,* Hiroshi Kiyono,† Hiromasa Hamada,* and Hiromichi Ishikawa[2]*

Through analysis of athymic (*nu/nu*) mice carrying a transgenic gene encoding GFP instead of RAG-2 product, it has recently been reported that, in the absence of thymopoiesis, mesenteric lymph nodes and Peyer's patches (PP) but not gut cryptopatches are pivotal birthplace of mature T cells such as the thymus-independent intestinal intraepithelial T cells (IEL). To explore and evaluate this important issue, we generated *nu/nu* mice lacking all lymph nodes (LN) and PP by administration of lymphotoxin-β receptor-Ig and TNF receptor 55-Ig fusion proteins into the timed pregnant *nu/+* mice that had been mated with male *nu/nu* mice (*nu/nu* LNP$^-$ mice). We also generated *nu/nu aly/aly* (*aly*, *alymphoplasia*) double-mutant mice that inherently lacked all LN, PP, and isolated lymphoid follicles. Although γδ-IEL were slightly smaller in number than those in *nu/nu* mice, substantial colonization of γδ-IEL was found to take place in the intestinal epithelia of *nu/nu* LNP$^-$ and *nu/nu aly/aly* mice. Notably, the population size of a major CD8αα$^+$ γδ-IEL subset was maintained, the use of TCR-γ-chain variable gene segments by these γδ-IEL was unaltered, and the development of cryptopatches remained intact in these *nu/nu* LNP$^-$ and *nu/nu aly/aly* mice. These findings indicate that all LN, including mesenteric LN, PP, and isolated lymphoid follicles, are not an absolute requirement for the development of γδ-IEL in athymic *nu/nu* mice. *The Journal of Immunology,* **2005, 174: 1906–1912.**

Over the past 2 decades, it has been revealed that numerous intestinal intraepithelial T cells (IEL)[3] have cellular and behavioral characteristics distinct from those of thymus-derived peripheral T cells (1–8). In mice, IEL are enriched with TCR-γδ T cells (γδ-IEL) (9, 10), and virtually all γδ-IEL and many αβ-IEL, unlike thymus-derived CD8αβ T cells that use the ζ-chain as part of their CD3 complex, express the unique CD8αα homodimer (11–14) and can use the FcRγ-chain in place of the ζ-chain (15–17). Along these findings, growing evidence has indicated thymus-independent (TI) development of such CD8αα-expressing IEL (TI-IEL) (5, 7, 11, 12, 18). Detection of RAG-1 and RAG-2 transcripts (12, 19–22) and identification of a small number of T-lineage-committed TCR$^-$ lymphocytes in IEL from wild-type mice (2, 12, 19, 20, 23–25) supported the concept of localized development of IEL in the epithelial layer in situ. However, it should be pointed out that the original view of extrathymic generation of CD8αα$^+$ αβ-IEL is now inconsistent with the results of recent studies in which the thymus-dependent generation of every αβ-IEL, including the CD8αα-expressing subset, is unequivocally demonstrated (26, 27).

Our search (28) for anatomical sites of IEL generation revealed multiple tiny clusters filled with ~1000 c-Kit$^+$IL-7R$^+$Lin$^-$ (Lin, lineage markers) lymphohemopoietic cells in the lamina propria (LP) of the intestinal crypt (cryptopatches (CP)). Data obtained through a series of CP studies strongly indicated that CP were essential sites for the extrathymic development of precursor T cells destined to become TI-IEL (22, 28–30). Specifically, the presence of both TCR-γ and -β germline transcripts in the c-Kit$^+$IL-7R$^+$Lin$^-$ CP lymphocytes (30) has emphasized that various DNA recombination enzymes are able to approach these chromosomal segments to commence the region-specific recombinations (31–33). On the whole, these findings lend strong support to the idea that T lineage-committed precursors, which match the developmental stage of triple-negative c-Kit^{high}CD44$^+$CD25$^{low/-}$ thymocytes before pre-Tα gene transcription (34, 35), but after expression of CD3ε-specific mRNA (35, 36), are present in gut CP (30). One impediment to this conclusion has been the detection of a marginal level of RAG-2 transcripts for CP lymphocytes (22). However, the analysis of athymic (*nu/nu*), bone marrow (BM) chimeric mice revealed that the development of donor BM-derived TI-IEL proceeded through several consecutive steps (30). BM-derived TCR$^-$ IEL first appeared within villous epithelia overlying the regenerated CP filled with BM-derived c-Kit$^+$IL-7R$^+$Lin$^-$ cells. These TCR$^-$ IEL subsequently emerged throughout the epithelia, and thereafter, conversion of TCR$^-$ to TCR$^+$ IEL, the final

*Department of Microbiology and Immunology, Keio University School of Medicine, and †Division of Mucosal Immunology, Department of Microbiology and Immunology, Institute of Medical Science, University of Tokyo, Tokyo, Japan; and ‡Department of Oral Medicine, Nihon University School of Dentistry, Chiba, Japan

Received for publication August 9, 2004. Accepted for publication December 10, 2004.

The costs of publication of this article were defrayed in part by the payment of page charges. This article must therefore be hereby marked *advertisement* in accordance with 18 U.S.C. Section 1734 solely to indicate this fact.

[1] This work was supported by Grant-in-Aid for Creative Scientific Research (13GS0015); the Japan Society for the Promotion of Science; a Grant-in-Aid for Scientific Research on Priority Areas A; a Grant-in-Aid for the 21st Century of Excellence Program entitled Understanding and Control of Life's Function via Systems Biology (Keio University); the Special Coordination Fund for Promoting Science and Technology, Ministry of Education, Culture, Sports, Science, and Technology; and Health Science Research Grants from the Ministry of Health, Labor, and Welfare.

[2] Address correspondence and reprint requests to Dr. Hiromichi Ishikawa, Department of Microbiology and Immunology, Keio University School of Medicine, Shinjuku-ku, Tokyo 160-8582, Japan. E-mail address: h-ishika@sc.itc.keio.ac.jp

[3] Abbreviations used in this paper: IEL, intestinal intraepithelial T cell; *aly*, alymphoplasia; BM, bone marrow; CP, cryptopatch; DN, double negative; iFABP, intestinal fatty acid-binding protein; IEC, intestinal epithelial cell; ILF, isolated lymphoid follicle; Lin, lineage marker; LNP$^-$, lymph node- and Peyer's patch deficient; LP, lamina propria; LT, lymphotoxin; LTβ-R, lymphotoxin-β receptor; MLN, mesenteric lymph node; PP, Peyer's patch; RORγt, retinoic acid-related orphan receptor; SCF, stem cell factor; Tg, transgenic; TI, thymus independent.

0022-1767/05/$02.00

step, took place very slowly. These results in conjunction with above-mentioned findings (2, 12, 19–25) have led us to conclude that TI-IEL complete their late maturational events, such as RAG-mediated TCR gene rearrangement, at a very slow rate in the epithelial layer in situ.

Recently, however, a new scenario for the extrathymic development of TI-IEL in *nu/nu* mice was described (37). By assessing RAG-2 expression in transgenic (Tg) *nu/nu* mice carrying a bacterial artificial chromosome encoding a GFP reporter instead of RAG-2, it was demonstrated that extrathymic T lymphopoiesis occurred mainly in mesenteric lymph nodes (MLN) and less in Peyer's patches (PP), but not in CP (37). To evaluate these new and important findings, we generated *nu/nu* mice that lacked all LN and PP by administration of lymphotoxin-β receptor (LTβ-R)-Ig and TNF-R55-Ig fusion proteins into pregnant *nu/+* mice (38) and double-mutant *nu/nu aly/aly* (*aly*, *alymphoplasia*) mice that lacked all LN, PP, as well as newly identified intestinal isolated lymphoid follicles (ILF) (39). We confirmed that these two kinds of mice harbored numerous $\gamma\delta$-IEL in the epithelial compartments of the small intestines and were found to retain gut CP. The significance of these findings is discussed from the viewpoint that all LN, PP, and ILF are dispensable anatomical sites for the generation of TI-IEL in the athymic *nu/nu* condition.

Materials and Methods

Mice

BALB/cA Jcl *nu/nu* (*nu/nu*), BALB/cA Jcl *nu/+* (*nu/+*), *aly/aly* Jcl mutant and C.B-17/Icr Jcl *scid/scid* (*scid/scid*) mice were purchased from CLEA Japan (Tokyo, Japan). TCR-$\gamma\delta$ (KN6)-Tg mice on the BALB/c background were described previously (40). Female KN6-Tg mice were crossed with *scid/scid* mice to generate KN6 *scid/+* mice, then they were backcrossed with *scid/scid* mice to obtain KN6 *scid/scid* mice. The presence of KN6-Tg was determined by PCR analysis of tail DNA with a set of primers to the KN6 Tg (5′-CAGATCCTTCCAGTTCATCC-3′ and 5′-CAGTCACTT GGGTTCCTTGTCC-3′), and the homozygous *scid/scid* genotype was determined by the absence of TCR-$\alpha\beta^+$ T cells in PBL. We generated transplacentally manipulated *nu/nu* and *nu/+* mice that lack all LN and PP according to essentially the same method described previously (38). In brief, timed-pregnant *nu/+* mice that had been mated with male *nu/nu* mice were i.v. injected with 200 μg of both LTβ-R-Ig and TNFR-55-Ig fusion proteins on gestational days 13 and 16. All mice used for experiments were between 8 and 18 wk of age, and absence of a thymus in various athymic mice was checked at necropsy. All animal procedures described in this study were performed in accordance with the guidelines for animal experiments of Keio University School of Medicine.

Production of nu/nu aly/aly *mice and genotyping of aly mutation*

Because *nu/nu* and *aly/aly* mothers are incapable of nursing the neonates, we used an in vitro fertilization technique (41) to produce (*nu/nu*×*aly/aly*)F_1 hybrid mice, then these heterozygous *nu/+ aly/+* mice were intercrossed to obtain *nu/nu aly/+*, *nu/nu aly/aly*, and *nu/+ aly/+ nu/+ aly/aly* littermates. To determine *aly/aly*, *aly/+*, and *+/+* alleles, the TaqMan assay of tail DNA was performed using the ABI PRISM 7000 sequence detection system (PerkinElmer) as previously described (42). The primer sequences for *aly* were 5′-GCCTACTGACATCCCGAGCTA-3′ (forward primer) and 5′-GCAGGACTGGGCTGGAAGA-3′ (reverse primer). The oligonucleotide probe corresponding mutant *aly* allele was 5′-AGACCG TACTGTTGAAG-3′ (FAM labeled), and the oligonucleotide probe corresponding wild-type allele was 5′-AGACCGTACCGTTGAA-3′ (VIC labeled). Underlining in sequences indicates point mutation. The 3′ end of each probe carried the quencher that suppressed the fluorescence of the reporter dyes. Each DNA sample was amplified with the TaqMan Universal master mixture containing AmpliTaq Gold DNA polymerase according to the manufacturer's instructions (Applied Biosystems). PCR conditions were 2 min at 50°C, 10 min at 95°C, 15 s at 95°C, and 1 min at 60°C for 40 cycles. During PCR, fluorescence developed when the oligonucleotide hybridized to perfectly matching DNA, and the exonuclease activity of *Taq* polymerase separated the quencher from the reporter dye. After PCR, the fluorescence yield for the two different dyes was measured and presented in a two-dimensional graph.

Antibodies

The following mAbs, described previously (22, 28–30, 39), were used. For immunohistochemical and immunofluorescence stainings: anti-$\gamma\delta$ (GL-3), anti-c-Kit (ACK-2), anti-B220 (RA3-6B2), and anti-IgA (C10-3) were used. For flow cytometric analysis, FITC-conjugated anti-$\alpha\beta$ (H57-597), anti-$\gamma\delta$ (GL-3), anti-Vγ1 (2.11; gift from Dr. S. Tonegawa, Center for Learning and Memory, MIT, Cambridge, MA), anti-Vγ4 (UC3-10A6), anti-Vγ7 (GL-1; gift from Dr. L. Lefrancois, Department of Medicine, Division of Immunology, University of Connecticut Health Center, Farmington, CT), anti-CD4 (GK 1.5), biotinylated anti-$\gamma\delta$ (GL-3), anti-B220 (RA3-6B2), anti-CD8α (53-6.7), and anti-c-kit (ACK-2), and PE-conjugated anti-CD8β (53-5.8) and anti-CD4 (GK 1.5) were used.

Immunohistochemical procedure

Longitudinally opened small intestine, ~10 mm in length, was pasted on a filter paper to form a horizontal section and then embedded in OCT compound (Tissue-Tek; Miles) at −80°C. The tissue segments were sectioned with a cryostat at 6 μm, and sections were preincubated with Block-Ace (Dainippon Pharmaceutical) to block nonspecific binding of mAbs. The sections were then incubated with hamster (anti-$\gamma\delta$) or rat (anti-c-Kit, anti-B220, or anti-IgA) mAb for 30 min at 37°C and rinsed three times with PBS, followed by incubation with biotin-conjugated goat anti-hamster IgG Ab (5 μg/ml; Cedarlane Laboratories) or with biotin-conjugated goat anti-rat IgG (5 μg/ml; Cedarlane Laboratories). Subsequently, the sections were washed three times with PBS, then incubated with avidin-biotin peroxidase complexes (Vectastain ABC kit; Vector Laboratories). Histochemical color development was achieved with Vectastain 3,3′-diaminobenzidine substrate kit (Vector Laboratories) according to the manufacturer's instructions. Finally, the sections were counterstained with hematoxylin for microscopy. Endogenous peroxidase activity was blocked with 0.3% H_2O_2 and 0.1% NaN_3 in distilled water for 10 min at room temperature. Tissue sections incubated with either nonimmune hamster serum or isotype-matched normal rat IgG showed only minimal background staining.

Immunofluorescence procedure

Tissue segments from thymus, spleen, inguinal LN, MLN, and PP from KN6 *scid/scid* mice were embedded in OCT compound at −80°C. The small intestine of KN6 *scid/scid* mice was longitudinally opened along the mesenteric wall, then intestine, ~10 mm in length, that had been rolled to form a vertical section was embedded in OCT compound at −80°C. Cryostat tissue sections, 6-μm thick, were fixed in acetone for 10 min at room temperature, washed three times with PBS, then pretreated with Block-Ace. Subsequently, the sections were incubated with anti-c-Kit mAb (ACK-2) for 60 min at 4°C, followed by incubation with PE-conjugated goat $F(ab')_2$ anti-rat IgG (H+L) (Invitrogen Life Technologies). The sections were then incubated with anti-$\gamma\delta$ mAb (GL-3) and counterstained with FITC-conjugated goat anti-hamster IgG (H+L) (Jackson ImmunoResearch Laboratories). Finally, the sections were examined under a fluorescence microscope (Axiovert 100; Carl Zeiss) equipped with an image analysis system (Signal Analytics).

Flow cytometry

IEL were isolated according to methods described previously (22). Lymphoid cells were incubated first with biotinylated mAb, then with streptavidin-PE (BD Biosciences) and FITC-conjugated second mAb. Stained cells were suspended in staining medium (Hanks' solution without phenol red, 0.02% NaN_3, and 2% heat-inactivated FBS) containing 0.5 μg/ml propidium iodide and analyzed using FACScan with CellQuest software (BD Biosciences). Dead cells were excluded by propidium iodide gating. Three-color analysis of IEL was also performed. IEL were incubated first with anti-CD8α mAb (biotinylated), then with streptavidin-Tri-Color (Caltag Laboratories). After washing, IEL were counterstained with two combinations of two PE-conjugated mAbs (anti-CD8β and anti-CD4 mAbs) and one FITC-conjugated mAb (anti-$\gamma\delta$), respectively. Lymphoid cells were incubated with anti-FcγR II/III mAb (2.4G2) before staining to block nonspecific binding of labeled mAbs to FcR.

Results

Development of $\gamma\delta$-IEL in nu/nu *mice is independent of all LN and PP*

To explore whether MLN are essential anatomical sites for the generation of TI-IEL in athymic *nu/nu* mice (37), we generated *nu/nu* mice that lacked all LN and PP. Pregnant *nu/+* female mice that had been mated with *nu/nu* male mice were injected with

LTβ-R-Ig and TNF-R55-Ig fusion proteins according to the protocol described by Rennert et al. (38), and the presence or the absence of LN and PP was determined in the progeny at 8 wk of age under a stereomicroscope. Although PP were absent from all treated mice, markedly attenuated remnants of MLN were present in about one-fifth of them. However, in every MLN-deficient *nu/nu* and *nu/+* offspring, the development of mandibular, axillary, inguinal, and popliteal (data not shown) LN (i.e., peripheral LN) and cervical (data not shown), iliac, and sacral LN (i.e., mucosal LN) was also ablated (LNP⁻ mice; Fig. 1).

Flow cytometric analysis of IEL isolated from *nu/nu*, *nu/nu* LNP⁻, *nu/+*, and *nu/+* LNP⁻ mice was performed using anti-TCR-αβ and anti-TCR-γδ mAbs. Consistent with well-established findings (3, 4, 8, 43), the proportion of αβ-IEL to γδ-IEL was sharply reduced, and the composition of IEL not expressing either type of TCR was expanded in athymic *nu/nu* conditions regardless of the presence or the absence of all LN and PP (Fig. 2*A*). In contrast, no significant differences in absolute numbers of IEL were observed between LNP⁻ and control LNP⁺ mice (data not shown). Notably, although the population size was slightly smaller by a factor of ~1.5 compared with that in IEL from control *nu/nu* mice, a large number of γδ-IEL was detected in IEL from *nu/nu* LNP⁻ mice (Fig. 2*A*). Compartmentalization of γδ-IEL within the epithelial layer of small intestine in *nu/nu* LNP⁻ mice was also verified by immunohistochemistry (Fig. 2*B*). These results indicate

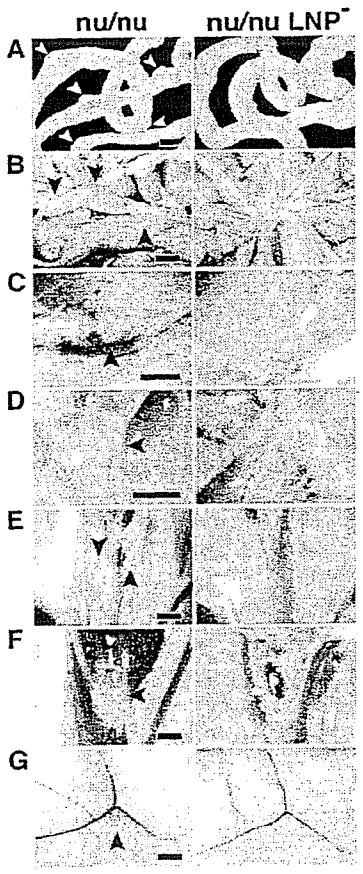

FIGURE 1. Development of PP and all LN in athymic *nu/nu* mice is ablated by in utero treatment with both LTβ-R-Ig and TNF-R55-Ig fusion proteins. PP (*A*), MLN (*B*), mandibular LN (*C*), axillary LN (*D*), iliac LN (*E*), sacral LN (*F*), and inguinal LN (*G*) are present in untreated *nu/nu* mice (arrowheads), but are undetectable in *nu/nu* mice that were treated in utero with both LTβ-R-Ig and TNF-R55-Ig fusion proteins (*nu/nu* LNP⁻ mice). Bar, 2 mm.

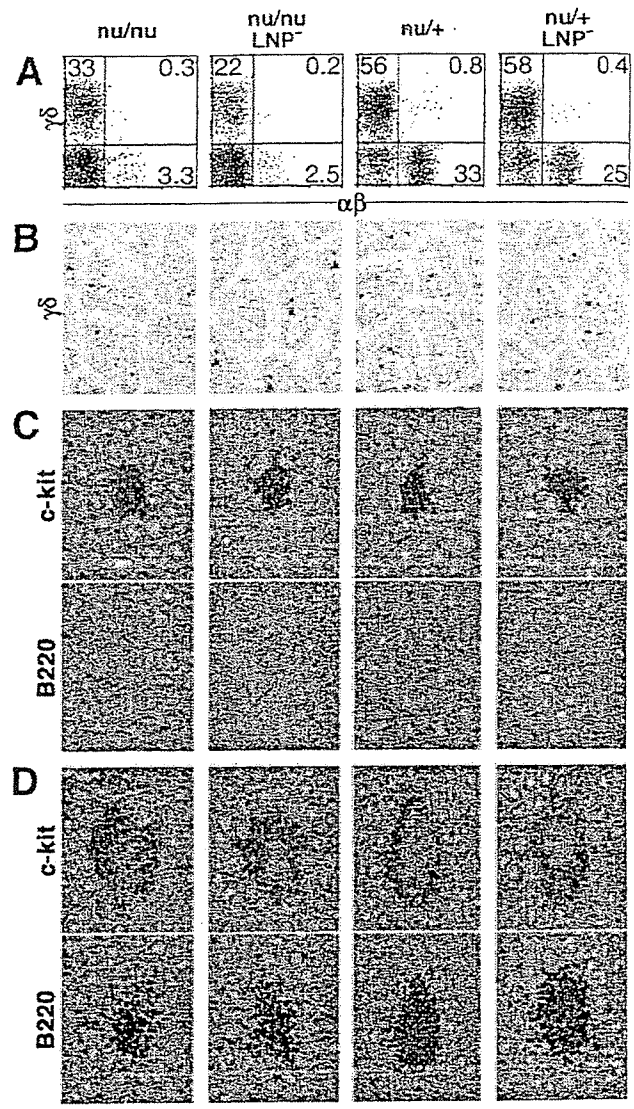

FIGURE 2. Flow cytometric analysis of IEL and immunohistochemical examination of small intestines from *nu/nu*, *nu/nu* LNP⁻, *nu/+*, and *nu/+* LNP⁻ mice. *A*, Although the population size of γδ-IEL in *nu/nu* LNP⁻ mice that lack all LN and PP is smaller than that of *nu/nu* mice, a substantial number of γδ-IEL are present in the epithelial compartment of *nu/nu* LNP⁻ mice, indicating that γδ-IEL are capable of developing in the absence of thymus, all LN including MLN, and PP. Note that the composition of αβ-IEL is reduced drastically in the athymic *nu/nu* condition compared with that in the euthymic *nu/+* condition. *B*, Representative immunohistochemical visualization of γδ-IEL in the small intestines of *nu/nu*, *nu/nu* LNP⁻, *nu/+*, and *nu/+* LNP⁻ mice (magnification, ×200). Although numbers of γδ-IEL in *nu/nu* LNP⁻ mice are decreased compared with those in *nu/nu* mice, colonization of γδ-IEL takes place in the absence of thymus, all LN including MLN, and PP (arrowheads). *C*, Representative immunohistochemical verification of CP in the small intestines of *nu/nu*, *nu/nu* LNP⁻, *nu/+*, and *nu/+* LNP⁻ mice (magnification, ×200). An average number and an approximate mass of CP filled with c-Kit⁺B200⁺ lymphocytes in these four different mice remain almost the same. *D*, Representative immunohistochemical verification of ILF in the small intestines of *nu/nu*, *nu/nu* LNP⁻, *nu/+*, and *nu/+* LNP⁻ mice (magnification, ×200). Note that a cluster of B220⁺ B cells that reside in the central region of ILF is surrounded by the layer of cells expressing c-Kit molecules.

that the development of γδ-IEL per se is independent of thymus, all LN, and PP.

With these findings in mind, we examined whether CP and ILF were present in these in utero manipulated LNP⁻ mice, because, in

contrast to PP that are already microscopically well developed just before birth (44), organogenesis of CP (28) and ILF (39) commences in early postnatal life. In fact, it was corroborated that the development of CP filled with closely packed c-Kit$^+$ lymphocytes (Fig. 2*C*) and ILF containing B220$^+$ B cell aggregation (Fig. 2*D*) remained intact in these *nu/nu* LNP$^-$ and *nu/+* LNP$^-$ mice.

Development of γδ-IEL in nu/nu aly/aly *double-mutant mice*

To ascertain the universality of the above findings, we explored the development of IEL in a mutant mouse that inherently lacked thymus, all LN, and PP, because fusion protein-treated LNP$^-$ mice might possess a minute and stereomicroscopically invisible MLN, even though this possibility appeared to be remote (38). With this purpose in mind, we generated *nu/nu aly/aly* double-mutant mice. In accordance with the earliest description (45), *nu/nu aly/aly* mice were devoid of all LN and PP (data not shown) as well as thymus. Importantly, substantial colonization of γδ-IEL in the small intestine of *nu/nu aly/aly* mice was verified by flow cytometric (Fig. 3*A*) and immunohistochemical (Fig. 3*B*) analyses. Furthermore, as inferred from our previous observations (28, 39), histogenesis of CP was detected (Fig. 3*C*), whereas development of ILF was completely blocked (Fig. 3*D*), in these double-mutant animals. Taking all of these results together (Figs. 2 and 3), neither thymus, all LN including MLN, PP, nor ILF is an absolute requirement for the development of γδ-IEL.

In this context, it is important to determine T and B cells and IgA$^+$ B cells that sojourn, respectively, in the spleen and LP of *nu/nu* LNP$^-$ and *nu/nu aly/aly* mice, because spleen is most likely the sole organized peripheral lymphoid tissue remaining in these animals, and *nu/nu aly/aly* mice lack intestinal IgA$^+$ B cell-producing plants such as PP and ILF. In contrast to abundant B220$^+$ B cells, mature T cells were virtually absent in the spleens of *nu/nu* LNP$^-$ (Fig. 4*A*) and *nu/nu aly/aly* (Fig. 4*C*) mice. In the small intestines, however, *nu/nu* LNP$^-$ mice possessed IgA$^+$ B cells (Fig. 4*B*), γδ-IEL, CP, and well-developed ILF (Fig. 2), whereas *nu/nu aly/aly* mice possessed γδ-IEL (Fig. 3, *A* and *B*) and CP (Fig. 3*C*), but lacked IgA$^+$ B cells (Fig. 4*C*) and ILF (Fig. 4*D*). These results indicate that all LN, including MLN, PP, and ILF, are not an absolute requirement for the generation of γδ-IEL in *nu/nu* mice and that the *aly* mutation interferes the formation of PP and ILF, resulting in the impaired development of IgA$^+$ B cells in villous LP.

Phenotypic and Vγ gene usage analyses of γδ-IEL in nu/nu *LNP$^-$ and* nu/nu aly/aly *mice*

The data reported to date indicate that γδ-IEL are potentially capable of developing in *nu/nu* mice lacking all LN, PP, and ILF. In this regard, however, it is reasonable to consider the possibility that γδ-IEL generated under such harsh conditions might differ from those generated in *nu/nu* mice possessing all LN, PP, and ILF. To address this issue, we conducted flow cytometric analysis of γδ-IEL isolated from *nu/nu*, *nu/nu* LNP$^-$, and *nu/nu aly/aly* mice. Although absolute numbers of γδ-IEL were lower by a factor of 2 compared with those in *nu/nu* mice (Fig. 5*A*), the composition of the major γδ-IEL subset expressing CD8αα homodimer (Fig. 5*A*) and the Vγ1, Vγ4, and Vγ7 gene segment used by such γδ-IEL (Fig. 5*B*) remained the same in both *nu/nu* LNP$^-$ and *nu/nu aly/aly* mice. Collectively, these results indicate that the absence of all LN, PP, and ILF exerts only a small effect on the phenotypic configuration of γδ-IEL in *nu/nu* mice.

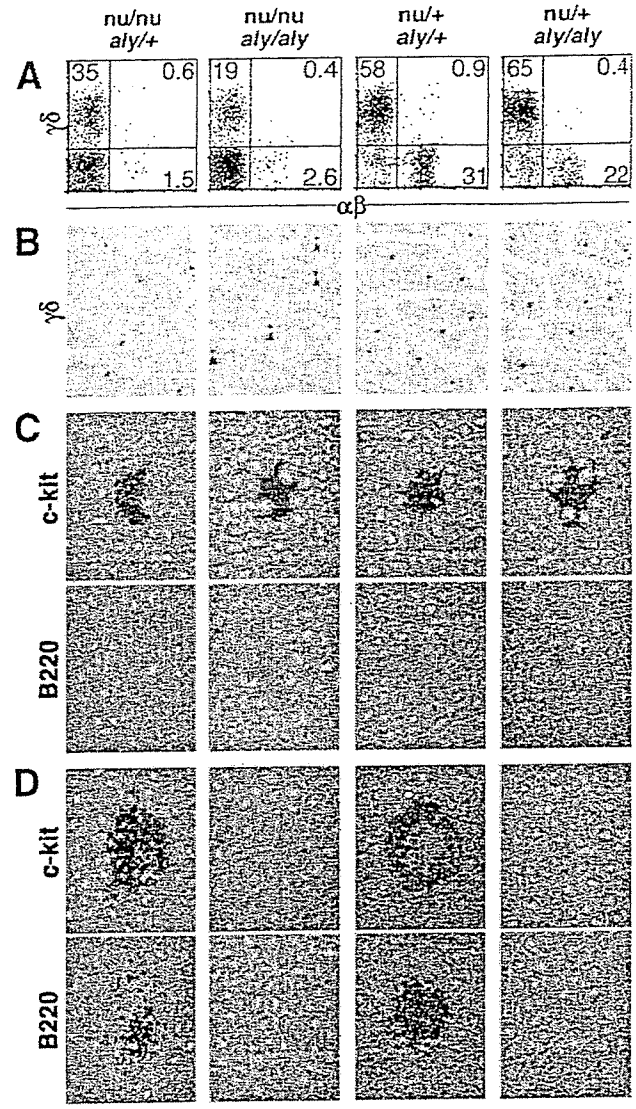

FIGURE 3. Flow cytometric analysis of IEL and immunohistochemical examination of small intestines from *nu/nu aly/+*, *nu/nu aly/aly*, *nu/+ aly/+*, and *nu/+ aly/aly* mice. *A*, Although the population size of γδ-IEL in *nu/nu aly/aly* mice that lack all LN, PP, and ILF is smaller than that in *nu/nu aly/+* mice, a significant number of γδ-IEL are present in the epithelial compartment of *nu/nu aly/aly* mice, indicating that γδ-IEL are capable of developing in the absence of thymus, all LN including MLN, PP, and ILF. Note that the composition of αβ-IEL is reduced drastically in the athymic *nu/nu* condition compared with that in the euthymic *nu/+* condition. *B*, Representative immunohistochemical verification of γδ-IEL in the small intestines of *nu/nu aly/+*, *nu/nu aly/aly*, *nu/+ aly/+*, and *nu/+ aly/aly* mice (magnification, ×200). Although numbers of γδ-IEL in *nu/nu aly/aly* mice are lower by a factor of 1.5–2 compared with those in *nu/nu aly/+* mice, a significant colonization of γδ-IEL takes place in the absence of thymus, all LN including MLN, PP, and ILF (arrowheads). *C*, Representative immunohistochemical verification of CP in the small intestines of *nu/nu aly/+*, *nu/nu aly/aly*, *nu/+ aly/+*, and *nu/+ aly/aly* mice (magnification, ×200). Although an average number of CP filled with c-Kit$^+$B220$^-$ lymphocytes in these four different mice remain almost the same, an approximate mass of CP present in *nu/nu aly/aly* and *nu/+ aly/aly* mice is slightly reduced compared with that of CP present in *nu/nu aly/+* and *nu/+ aly/+* mice. *D*, Representative immunohistochemical verification of ILF in the small intestines of *nu/nu aly/+*, *nu/nu aly/aly*, *nu/+ aly/+*, and *nu/+ aly/aly* mice (magnification, ×200). Note that ILF are undetectable throughout the small intestinal mucosa of *nu/nu aly/aly* and *nu/+ aly/aly* mice.

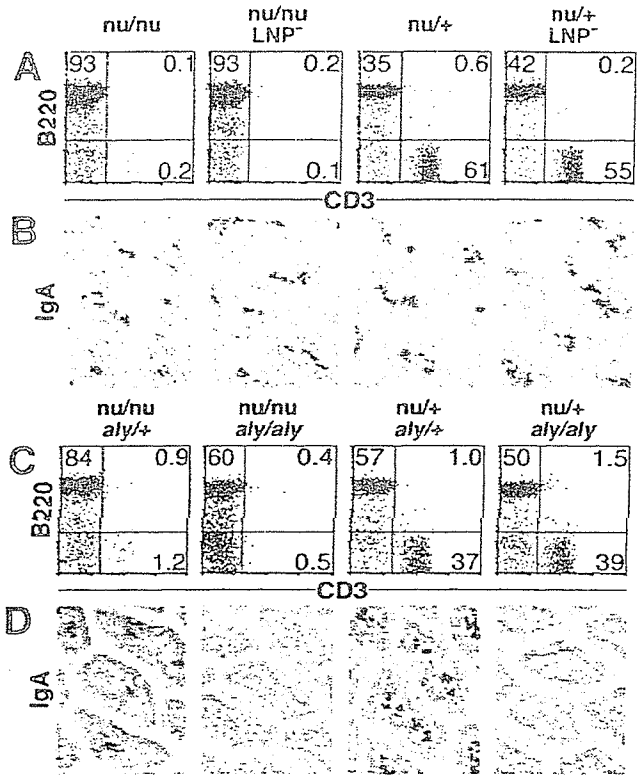

FIGURE 4. Flow cytometric analysis of splenic T and B cells and immunohistochemical verification of intestinal IgA$^+$ B cells in *nu/nu*, *nu/nu* LNP$^-$, *nu/nu aly/+*, and *nu/nu aly/aly* mice. *A*, Although mature CD3$^+$ T cells are nearly absent from the spleens of *nu/nu* and *nu/nu* LNP$^-$ mice, abundant B220$^+$ B cells are detected in the spleens of these athymic animals. Colonization of IgA$^+$ B cells in the villous LP of *nu/nu*, *nu/nu* LNP$^-$, *nu/+*, and *nu/+* LNP$^-$ mice is comparable. *B*, Only a marginal number of mature CD3$^+$ T cells are detected in the spleens of *nu/nu aly/+* and *nu/nu aly/aly* mice, and a large fraction of the remaining lymphoid cells consists of B220$^+$ B cells. In contrast, villous LP of *nu/nu aly/aly* and *nu/+ aly/aly* mice has no IgA$^+$ B cells.

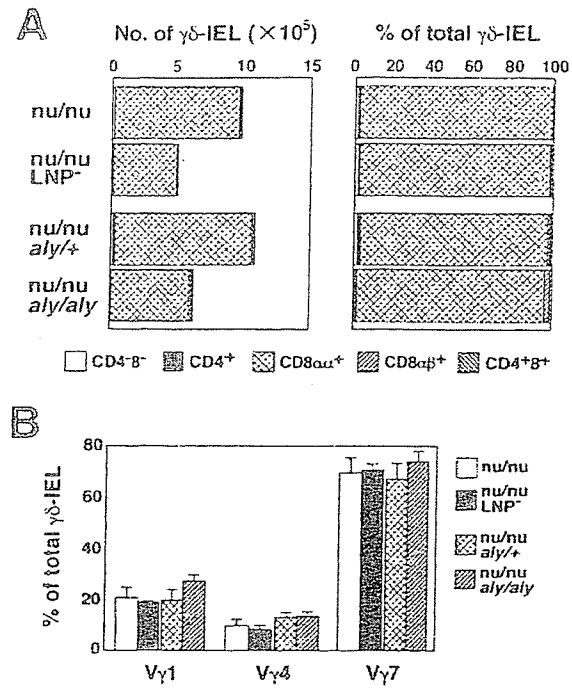

FIGURE 5. Flow cytometric analysis of γδ-IEL from *nu/nu*, *nu/nu* LNP$^-$, nu/nu *aly/+*, and *nu/nu aly/aly* mice and Vγ gene segments used by γδ-IEL in these athymic *nu/nu* mice. *A*, Three-color analysis was performed. Absolute numbers of double-negative (CD4$^-$8$^-$), single-positive (CD4$^+$, CD8αα$^+$, or CD8αβ$^+$), and double-positive (CD4$^+$8$^+$) subsets in the γδ-IEL population were calculated on the basis of total numbers of γδ-IEL. Data are the mean values from five mice per group. *B*, Two-color analysis was performed. IEL isolated from these *nu/nu* mice were incubated first with anti-TCR-γδ mAb (biotinylated), then with streptavidin-PE and FITC-conjugated anti-Vγ1, anti-Vγ4, or anti-Vγ7 mAb. The results are the mean ± SD of data obtained from four mice per group.

Development of c-Kit$^+$ γδ-IEL in scid/scid *mice expressing Tg TCR-γδ*

We have shown that IL-7 produced by intestinal epithelial cells (IEC) is important for intraintestinal development of γδ-IEL and is crucial for organization of intestinal mucosal lymphoid tissues, such as PP and CP (18). It has also been shown that c-Kit and stem cell factor (SCF) are expressed by γδ-IEL and IEC, respectively, and signaling through c-Kit/SCF is indispensable for normal development of γδ-IEL (46, 47). Thus, these previous (46, 47) and the present findings in conjunction with results obtained with BM chimeric mice (30), reinforce the idea that the development of γδ-IEL takes place in the intestinal mucosa in situ. In an attempt to confirm and visualize directly the cellular events that proceed toward gut-oriented γδ-IEL generation, i.e., c-Kit$^+$ CP cells→c-Kit$^+$ TCR-γδ T cells→c-Kit$^-$ γδ-IEL, we generated *scid/scid* mice expressing KN6-Tg TCR-γδ (48). Double-immunofluorescence analysis of small intestinal tissues containing CP highlighted these presumptive cellular events. Thus, a representative picture of jejunal tissue sections from KN6 *scid/scid* mice (Fig. 6*A*) shows that a cluster of c-Kit$^+$ cells in a CP (red) does not express TCR-γδ, and that large numbers of γδ-IELs (green) are present in the epithelial layer, especially in the epithelium adjacent to CP. Notably, quite a large number of lymphocytes expressing both c-Kit and TCR-γδ molecules (yellow or orange) is also present in the epithelial and LP compartments of villi (Fig. 6*A*). Neither clustering c-Kit$^+$ cells nor lymphocytes stained yellow/orange were detected in other lymphoid tissues, such as thymus, LN, PP, and spleen (data not shown). Flow cytometric analysis of cell surface c-Kit molecules on the gated γδ T cells confirmed that a large fraction of γδ-IEL was c-Kit positive, namely, double-positive TCR-γδ$^+$c-Kit$^+$ cells (Fig. 6*B*, *upper panel*). In contrast, abundant Tg γδ T cells residing in MLN, spleen, and thymus did not include such c-Kit-expressing, double-positive cells (Fig. 6*B*, *lower three panels*). Overall, these results support the above-described basic premise that the development of γδ-IEL takes place in the intestinal mucosa in situ. However, because KN6-Tg TCR-γδ-expressing cells have not been detected in the CP of KN6 *scid/scid* mice (Fig. 6*A*), whether CP are essential and indispensable anatomical sites in generating γδ-IEL remained highly contentious.

Discussion

Because most of the numerous lymphocytes residing in the murine IEC compartment unexpectedly turned out to be T cells (IEL), additional revelation toward the end of the last century indicated that they display phenotypic and functional characteristics distinct from those of other T cell populations and that their development does not necessarily depend on the thymus (TI-IEL) (1–18). Likewise, several lines of information have illuminated the distinctive T cell facets of human fetal intestine (49, 50), and on the basis of RAG expression, there may also be TI-IEL that develop in human (51, 52) and rat (53) intestines. Although evidence for the vestigial lymphocyte-producing function of gut mucosa is substantial, as mentioned above (2, 5, 7, 11, 12, 18–25, 49–53), recent studies

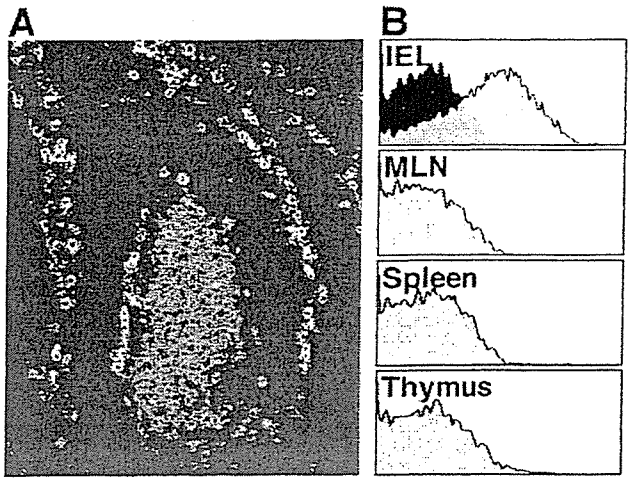

FIGURE 6. Double immunofluorescence analysis of small intestinal tissues containing CP and flow cytometric analysis of lymphocytes from KN6 *scid/scid* mice. *A*, Intestinal birthplace of intraepithelial γδ T cells (magnification, ×400). A cluster of lymphocytes in a CP is positively stained with anti-c-Kit mAb (PE), but not with anti-γδ mAb (FITC), resulting in a red color. Conversely, many IEL, especially those adjacent to CP, are positively stained with anti-γδ mAb (FITC), but not with anti-c-Kit mAb (PE), resulting in a green color. Note that a large number of lymphocytes present in the epithelial and LP compartments of villi are positively stained with anti-c-Kit mAb (PE) and anti-γδ mAb (FITC), resulting in a yellow or orange color. Neither the clusters filled with c-Kit$^+$ cells nor lymphocytes stained yellow or orange are detected in the other lymphoid organs, such as thymus, LN, and spleen. *B*, Expression of c-Kit molecules by Tg γδ T cells that colonize in the intestinal epithelial, MLN, and splenic and thymic compartments of KN6 *scid/scid* mice. IEL, MLN cells, spleen cells, and thymocytes were incubated first with anti-TCR-γδ mAb (biotinylated), then with streptavidin-PE and FITC-conjugated anti-c-Kit mAb. Profiles of c-Kit expression by the gated TCR-γδ$^+$ cell population are presented. The *dark area* in the *upper panel* depicts a FITC-positive cell profile of IEL that were stained simply with biotinylated anti-TCR-γδ mAb and streptavidin-PE (negative control). It is evident that IEL contain a large number of double-positive (TCR-γδ$^+$ c-Kit$^+$) cells, but that MLN, spleen, and thymus have no such double-positive cells.

have made it clear that CD8αα does not serve as a marker for TI development of αβ-IEL (26, 27). In contrast, because positive and/or negative selection of TCR-γδ T cells in the thymus is not as evident (26, 27), thymic dependency for functional TCR-γδ T cells is less obvious.

In an assessment of the expression of Tg-encoded GFP in place of RAG-2 protein, no evidence was obtained for a lymphopoietic process involving CP cells migrating into gut epithelium to undergo TCR gene rearrangement and maturation into αβ- and γδ-IEL even in the athymic *nu/nu* condition (37). Instead, MLN and, less efficiently, PP have been identified as the major extrathymic T cell-producing plants in athymic *nu/nu* mice, and the newly generated T cells migrate from MLN into thoracic duct lymph to reach the gut epithelia, indicating that MLN and PP are the pivotal sites in generating TI-IEL, mostly γδ-IEL (37). In this context, the development of γδ-IEL should be hampered in *nu/nu* mice that simultaneously lack MLN and PP. Our present findings argue against this scenario by showing that not only transplacentally manipulated *nu/nu* LNP$^-$ mice lacking all LN and PP, but also genetically defined *nu/nu aly/aly* mice lacking all LN, PP, and ILF harbor a substantial population of γδ-IEL (Fig. 2, *A* and *B*, and Fig. 3, *A* and *B*), although these two different mouse models may share the same confounding factors. In contrast to what was observed in *nu/nu* mice, the extrathymic pathway of IEL generation was shown to be totally repressed in the euthymic condition using the same GFP RAG-2 Tg mouse model (37). The authors proposed that all IEL, including CD8αα$^+$ IEL, in normal mice were the likely progeny of double-negative (DN) TCR-αβ$^-$ and -γδ$^+$ thymocytes and noted that extremely complex and unusual T cell characteristics of murine IEL with respect to their expression of various accessory, costimulation, activation, and adhesion markers (4, 5) might be brought about by the distinctive microenvironment of gut epithelium (37). In this context, for instance, many DN thymocytes somehow down-regulate cell surface expression of Thy-1 molecules, because a substantial fraction of IEL is Thy-1 negative, whereas most of them must up-regulate c-Kit molecules on the way to becoming IEL (46, 47) (Fig. 6). Even if all of those transfigurations (>20) are attributable to the inherent properties of gut epithelium, the biological significance as well as the molecular level of the mechanisms underlying such enigmatic cellular events remain highly contentious. It should also be pointed out that our recent findings (18) are inconsistent with this idea (37). γδ T cells are absent in IL-7$^{-/-}$ mice due to the selective blockade of TCR-γ gene rearrangements (54). Using the intestinal fatty acid-binding protein (iFABP) promoter, we reinstated the expression of IL-7 to mature IEC of IL-7$^{-/-}$ mice (iFABP-IL7) (18). Although γδ-IEL were restored in iFABP-IL7 mice as well as CP and PP, γδ T cells remained absent from all tissues, including thymus, spleen, and skin. These results clearly indicate that γδ-IEL generated in iFABP-IL7 mice are not of DN TCR-γδ$^+$ thymocyte origin and that the recombination of TCR-γ genes in TCR-precursor T cells takes place in situ with the assistance of IL-7 produced locally by IEC.

Our present findings provide compelling evidence for the development of γδ-IEL within the intestine of *nu/nu* mice that lack the thymus, all LN, PP, and ILF. It should be pointed out, however, that the population size and absolute numbers of γδ-IEL from *nu/nu* LNP$^-$ and *nu/nu aly/aly* mice are smaller than those from the corresponding control *nu/nu* mice (Figs. 2*A*, 3*A*, and 5*A*). These features would indicate that LN and PP, in fact, contribute to γδ-IEL numbers in the *nu/nu* condition. In contrast to the results obtained in GFP RAG-2 Tg mouse model (37), our previous RT-PCR analysis of lymphocytes from normal euthymic mice showed that under conditions in which mRNA from 50 thymocytes displayed a strong signal for RAG-2 transcripts and mRNA from 6250 RAG-2$^{-/-}$ thymocytes failed to display any detectable signals, very low levels of RAG-2 transcripts were constantly detected in an amount of mRNA equivalent to 6250 IEL and CP cells (22). These findings suggest that a small minority of IEL and possibly CP cells also is undergoing TCR gene rearrangement, that they are able to do so with a minimum amount of RAG-2 transcripts, or both. Actually, we still do not know how many RAG-1 and -2 molecules per nucleus are required to drive the region-specific V(D)J recombinations of TCR genes. It is possible that the amount of mRNA encoding RAG-1 and -2 molecules required by thymocytes for the successful recombination of TCR genes may not be that large. It should also be pointed out that using cell fate mapping, almost all αβ-IEL have recently been shown to be the progeny of immature CD4$^+$CD8$^+$ thymocytes (55). Furthermore, by using elegant and sophisticated approaches (55), it has been revealed that the retinoic acid-related orphan receptors (RORγt) detected in fetal lymphoid tissue-inducer cells are also expressed in cells within gut CP, and that γδ-IEL are not the progeny of such RORγt-positive CP lymphocytes. Specifically, however, it has remained an open question whether a small, but significant, fraction of lymphocytes in CP does not retain RORγt molecules or whether almost all CP lymphocytes express RORγt (55). In any event, to substantiate the intraintestinal development of γδ-IEL in these *nu/nu* LNP$^-$ and *nu/nu aly/aly* mice, clear identification of T cells

undergoing TCR gene rearrangement in the gut mucosa appears to be of critical importance.

Acknowledgments

We are grateful to Dr. L. Lefrancois for his critical reading of the manuscript. We thank N. Hosaka and M. Mori for their excellent technical assistance.

References

1. Rocha, B., D. Guy-Grand, and P. Vassalli. 1995. Extrathymic T cell differentiation. *Curr. Opin. Immunol. 7:235.*
2. Mowat, A. M., and J. L. Viney. 1997. The anatomical basis of intestinal immunity. *Immunol. Rev. 156:145.*
3. Klein, J. R. 1998. Thymus-independent development of gut T cells. *Chem. Immunol. 71:88.*
4. Lefrancois, L., and L. Puddington. 1999. Basic aspects of intraepithelial lymphocyte immunobiology. In *Mucosal Immunology.* P. L. Ogra, J. Mestecky, M. E. Lamm, W. Strober, J. Bienenstock, and J. R. McGhee, eds. Academic Press, San Diego, p. 413.
5. Aranda, R., B. C. Sydora, and M. Kronenberg. 1999. Intraepithelial lymphocytes: function. In *Mucosal Immunology.* P. L. Ogra, J. Mestecky, M. E. Lamm, W. Strober, J. Bienenstock, and J. R. McGhee, eds. Academic Press, San Diego, p. 429.
6. Poussier, P., and M. Julius. 1999. Speculation on the lineage relationships among $CD4^-8^+$ gut-derived T cells and their role(s). *Semin. Immunol. 11:293.*
7. Hayday, A., E. Theodoridis, E. Ramsburg, and J. Shires. 2001. Intraepithelial lymphocytes: exploring the Third Way in immunology. *Nat. Immunol. 2:997.*
8. Guy-Grand, D., and P. Vassalli. 2002. Gut intraepithelial lymphocyte development. *Curr. Opin. Immunol. 14:255.*
9. Goodman, T., and L. Lefrancois. 1988. Expression of the γ-δ T-cell receptor on intestinal $CD8^+$ intraepithelial lymphocytes. *Nature 333:855.*
10. Bonneville, M., C. A. Janeway, K. Ito, W. Haser, I. Ishida, N. Nakanishi, and S. Tonegawa. 1988. Intestinal intraepithelial lymphocytes are a distinct set of γδ T-cells. *Nature 336:479.*
11. Lefrancois, L. 1991. Phenotype complexity of intraepithelial lymphocyte of the small intestine. *J. Immunol. 147:1746.*
12. Guy-Grand, D., N. Cerf-Bensussan, B. Malissen, M. Malassis-Seris, C. Briottet, and P. Vassalli. 1991. Two gut intraepithelial $CD8^+$ lymphocyte populations with different T cell receptors: a role for the gut epithelium in T cell differentiation. *J. Exp. Med. 173:471.*
13. Maloy, K. J., A. M. Mowat, R. Zamoyska, and I. N. Crispe. 1991. Phenotypic heterogeneity of intraepithelial T lymphocytes from mouse small intestine. *Immunology 72:555.*
14. Kawaguchi, M., M. Nanno, Y. Umesaki, S. Matsumoto, Y. Okada, Z. Cai, T. Shimamura, Y. Matsuoka, M. Ohwaki, and H. Ishikawa. 1993. Cytolytic activity of intestinal intraepithelial lymphocytes in germ-free mice is strain dependent and determined by T cells expressing γδ T-cell antigen receptors. *Proc. Natl. Acad. Sci. USA 90:8591.*
15. Malissen, M., A. Gillet, B. Rocha, J. Trucy, E. Vivier, C. Boyer, F. Kontgen, N. Brun, G. Mazza, E. Spanopoulou, et al. 1993. T cell development in mice lacking CD3-ζ/η gene. *EMBO J. 12:4347.*
16. Ohno, H., T. Aoe, S. Taki, D. Kitamura, Y. Ishida, K. Rajewsky, and T. Saito. 1993. Development and functional impairment of T cells in mice lacking CD3ζ chains. *EMBO J. 12:4357.*
17. Liu, C-P., R. Ueda, J. She, J. Sancho, B. Wang, G. Weddell, J. Loring, C. Kurahara, E. C. Dudley, A. Hayday, et al. 1993. Abnormal T cell development in $CD3\zeta^{-/-}$ mutant mice and identification of a novel T cell population in the intestine. *EMBO J. 12:4863.*
18. Laky, K., L. Lefrancois, E. G. Lingenheld, H. Ishikawa, J. M. Lewis, S. Olson, K. Suzuki, R. E. Tigelaar, and L. Puddington. 2000. Enterocyte expression of IL-7 induces development of γδ T cells and Peyer's patches. *J. Exp. Med. 191:1569.*
19. Guy-Grand, D., C. V. Broecke, C. Briottet, M. Malassis-Seris, F. Selz, and P. Vassalli. 1992. Different expression of the recombination activity gene RAG-1 in various populations of thymocytes, peripheral T cells and gut thymus-independent intraepithelial lymphocytes suggests two pathways of T cell receptor rearrangement. *Eur. J. Immunol. 22:505.*
20. Lin, T., G. Matsuzaki, H. Yoshida, N. Kobayashi, H. Kenai, K. Omoto, and K. Nomoto. 1994. $CD3^-CD8^+$ intestinal intraepithelial lymphocytes (IEL) and the extrathymic development of IEL. *Eur. J. Immunol. 24:1080.*
21. Boll, G., A. Rudolphi, S. Spieb. and J. Reimann. 1995. Regional specialization of intraepithelial T cells in the murine small and large intestine. *Scand. J. Immunol. 41:103.*
22. Oida, T., K. Suzuki, M. Nanno, Y. Kanamori, H. Saito, E. Kubota, S. Kato, M. Itoh, S. Kaminogawa, and H. Ishikawa. 2000. Role of gut cryptopatches in early extrathymic maturation of intestinal intraepithelial T cells. *J. Immunol. 164:3616.*
23. Hamad, M., M. Whetsell, J. Wang, and J. R. Klein. 1997. T cell progenitors in the murine small intestine. *Dev. Comp. Immunol. 21:435.*
24. Page, S. T., L. Y. Bogatzki, J. A. Hamerman, C. H. Sweenie, P. J. Hogarth, M. Malissen, R. M. Perlmutter, and A. M. Pullen. 1998. Intestinal intraepithelial lymphocytes include precursors committed to the T cell receptor αβ lineage. *Proc. Natl. Acad. Sci. USA 95:9459.*
25. Woodward, J., and E. Jenkinson. 2001. Identification and characterization of lymphoid precursors in the murine intestinal epithelium. *Eur. J. Immunol. 31:3329.*
26. Leishman, A. J., L. Gapin, M. Capone, E. Palmer, H. R. MacDonald, M. Kronenberg, and H. Cheroutre. 2002. Precursors of functional MHC class I- or class II-restricted $CD8\alpha\alpha^+$ T cells are positively selected in the thymus by agonist self-peptides. *Immunity 16:355.*
27. Cheroutre, H. 2004. Starting at the beginning: new perspectives on the biology of mucosal T cells. *Annu. Rev. Immunol. 22:217.*
28. Kanamori, Y., K. Ishimaru, M. Nanno, K. Maki, K. Ikuta, H. Nariuchi, and H. Ishikawa. 1996. Identification of novel lymphoid tissues in murine intestinal mucosa where clusters of $c\text{-}kit^+$ $IL\text{-}7R^+$ $Thy1^+$ lympho-hemopoietic progenitors develop. *J. Exp. Med. 184:1449.*
29. Saito, H., Y. Kanamori, T. Takemori, H. Nariuchi, E. Kubota, H. Takahashi-Iwanaga, T. Iwanaga, and H. Ishikawa. 1998. Generation of intestinal T cells from progenitors residing in gut cryptopatches. *Science 280:275.*
30. Suzuki, K., T. Oida, H. Hamada, O. Hitotsumatsu, M. Watanabe, T. Hibi, H. Yamamoto, E. Kubota, S. Kaminogawa, and H. Ishikawa. 2000. Gut cryptopatches: direct evidence of extrathymic anatomical sites for intestinal T lymphopoiesis. *Immunity 13:691.*
31. Alt, F. W., T. K. Blackwell, and G. D. Yancopoulos. 1987. Development of the primary antibody repertoire. *Science 238:1079.*
32. Hempel, W. M., I. Leduc, N. Mathieu, R. K. Tripathi, and P. Ferrier. 1998. Accessibility control of V(D)J recombination: lessons from gene targeting. *Adv. Immunol. 69:309.*
33. Ye, S.-K., K. Maki, T. Kitamura, S. Sunaga, K. Akashi, J. Domen, I. L. Weissman, T. Honjo, and K. Ikuta. 1999. Induction of germline transcription in the TCRγ locus by Stat5: implications for accessibility control by the IL-7 receptor. *Immunity 11:213.*
34. Saint-Ruf, C., K. Ungewiss, M. Groettrup, L. Bruno, H. J. Fehling, and H. von Boehmer. 1994. Analysis and expression of a cloned pre-T cell receptor gene. *Science 266:1208.*
35. Wilson, A., and H. R. MacDonald. 1995. Expression of genes encoding the pre-TCR and CD3 complex during thymus development. *Int. Immunol. 7:1659.*
36. Wang, B., N. Wang, C. E. Whitehurst, J. She, J. Chen, and C. Terhorst. 1999. T lymphocyte development in the absence of CD3ε or CD3γδε*ζ*. *J. Immunol. 162:88.*
37. Guy-Grand, D., O. Azogui, S. Celli, S. Darche, M. C. Nussenzweig, P. Kourilsky, and P. Vassalli. 2003. Extrathymic T cell lymphopoiesis: ontogeny and contribution to gut intraepithelial lymphocytes in athymic and euthymic mice. *J. Exp. Med. 197:333.*
38. Rennert, P. D., D. James, F. Mackay, J. L. Browning, and P. S. Hochman. 1998. Lymph node genesis is induced by signaling through the lymphotoxin β receptor. *Immunity 9:71.*
39. Hamada, H., T. Hiroi, Y. Nishiyama, H. Takahashi, Y. Masunaga, S. Hachimura, S. Kaminogawa, H. Takahashi-Iwanaga, T. Iwanaga, H. Kiyono, et al. 2002. Identification of multiple isolated lymphoid follicles on the antimesenteric wall of the mouse small intestine. *J. Immunol. 168:57.*
40. Kawaguchi-Miyashita, M., S. Shimada, H. Kurosu, N. Kato-Nagaoka, Y. Matsuoka, M. Ohwaki, H. Ishikawa, and M. Nanno. 2001. An accessory role of TCR-$\gamma\delta^+$ cells in the exacerbation of inflammatory bowel disease in TCRα mutant mice. *Eur. J. Immunol. 31:980.*
41. Hogan, B., F. Costantini, and E. Lacy. 1986. Recovery, culture, and transfer of embryo. In *Manipulating the Mouse Embryo.* B. Hogan, F. Costantini, and E. Lacy, eds. Cold Spring Harbor Laboratory, Plainview, p. 90.
42. Ranade, K., M.-S. Chang, C.-T. Ting, D. Pei, C.-F. Hsiao, M. Olivier, R. Pesich, J. Hebert, Y.-D. Chen, V. J. Dzau, et al. 2001. High-throughput genotyping with single nucleotide polymorphisms. *Genome Res. 11:1262.*
43. Lefrancois, L., and S. Olson. 1997. Reconstitution of the extrathymic intestinal T cell compartment in the absence of irradiation. *J. Immunol. 159:538.*
44. Yoshida, H., K. Honda, R. Shinkura, S. Adachi, S. Nishikawa, K. Maki, K. Ikuta, and S.-I. Nishikawa. 1999. IL-7 receptor α^+ $CD3^-$ cells in the embryonic intestine induces the organizing center of Peyer's patches. *Int. Immunol. 11:643.*
45. Miyawaki, S., Y. Nakamura, H. Suzuka, M. Koba, R. Yasumizu, S. Ikehara, and Y. Shibata. 1994. A new mutation, aly, that induces a generalized lack of lymph nodes accompanied by immunodeficiency in mice. *Eur. J. Immunol. 24:429.*
46. Puddington, L., S. Olson, and L. Lefrancois. 1994. Interactions between stem cell factor and c-Kit are required for intestinal immune system homeostasis. *Immunity 1:733.*
47. Laky, K., L. Lefrancois, and L. Puddington. 1997. Age-dependent intestinal lymphoproliferative disorder due to stem cell factor deficiency. Parameters in small and large intestine. *J. Immunol. 158:1417.*
48. Ishida, I., S. Verbeek, M. Bonneville, S. Itohara, A. Berns, and S. Tonegawa. 1990. T cell receptor γδ and γ transgenic mice suggest a role of a γ gene silencer in the generation of αβ T cells. *Proc. Natl. Acad. Sci. USA 87:3067.*
49. Koningsberger, J. C., A. Chott, T. Logtenberg, L. J. Wiegman, R. S. Blumberg, G. P. van Berge Henegouwen, and S. P. Balk. 1997. TCR expression in human fetal intestine and identification of an early T cell receptor β-chain transcript. *J. Immunol. 159:1775.*
50. Howie, D., J. Spencer, D. DeLord, C. Pitzalis, N. C. Wathen, A. Dogan, A. Akbar, and T. T. MacDonald. 1998. Extrathymic T cell differentiation in the human intestine early in life. *J. Immunol. 161:5862.*
51. Lundqvist, C., V. Baranov, S. Hammarstrom, L. Athlin, and M.-L. Hammarstrom. 1995. Intra-epithelial lymphocytes: evidence for regional specialization and extrathymic T cell maturation in the human gut epithelium. *Int. Immunol. 7:1473.*
52. Lynch, S., D. Kelleher, R. McManus, and C. O'Farrelly. 1995. RAG1 and RAG2 expression in human intestinal epithelium: evidence of extrathymic T cell differentiation. *Eur. J. Immunol. 25:1143.*
53. Ramanathan, S., L. Marandi, and P. Poussier. 2002. Evidence for the extrathymic origin of intestinal TCR $\gamma\delta^+$ T cells in normal rats and for an impairment of this differentiation pathway in BB rats. *J. Immunol. 168:2182.*
54. Maki, K., S. Sunaga, and K. Ikuta. 1996. The V-J recombination of T cell receptor-γ genes is blocked in interleukin-7 receptor-deficient mice. *J. Exp. Med. 184:2423.*
55. Eberl, C., and D. R. Littman. 2004. Thymic origin of intestinal αβ T cells revealed by fate mapping of $ROR\gamma t^+$ cells. *Science 305:248.*

Available online at www.sciencedirect.com
SCIENCE DIRECT®
Biochemical and Biophysical Research Communications 331 (2005) 285–294
BBRC
www.elsevier.com/locate/ybbrc

Triggering of TLR3 by polyI:C in human corneal epithelial cells to induce inflammatory cytokines

Mayumi Ueta [a,*], Junji Hamuro [a], Hiroshi Kiyono [b], Shigeru Kinoshita [a]

[a] *Department of Ophthalmology, Kyoto Prefectural University of Medicine, Kyoto, Japan*
[b] *Division of Mucosal Immunology, The Institute of Medical Science, The University of Tokyo, 4-6-1 Shirokanedai, Minato-ku, Tokyo, Japan*

Received 23 February 2005
Available online 1 April 2005

Abstract

Epithelial cells of the ocular surface are key in the first-line defense as a part of the mucosal immune system against pathogens. We investigated whether polyI:C induces the production by human corneal epithelial cells (HCEC) of pro-inflammatory cytokines and IFN-β, and whether Toll-like receptor (TLR)-3 expression is amplified by polyI:C. TLR3 was expressed on the surface of HCEC. Stimulation with polyI:C elicited the elevated production and mRNA expression of IL-6 and IL-8 in HCEC. While polyI:C induced IFN-β, far stronger than human fibroblasts, and TLR3 gene expression in HCEC, LPS stimulation did not. Similarly, polyI:C, but not LPS, induced the gene expression of IκBα and MAIL, members of the IκB family, in HCEC. The innate immune response of HCEC is distinct from that of immune-competent cells, and we suggest that this is indicative of the symbiotic relationship between corneal epithelium and microbes inhabiting the ocular surface.

Keywords: Human corneal epithelial cells; PolyI:C; TLRs; Inflammation; LPS

On the ocular surfaces as in the intestine, the surface epithelium serves a critical function in the front-line defense of the mucosal innate immune system [1–3]. Upon challenge, epithelial cells lining mucosal surfaces play a pivotal role in innate immunity by secreting chemokines and other immune mediators. The ability to detect microbes is arguably the most important task of the immune system. Exaggerated host defense reaction of the epithelium to endogenous bacteria may induce the initiation and perpetuation of inflammatory mucosal responses [4–6].

The ability of cells to recognize microbial motifs and pathogen associated molecular patterns (PAMPs) rests on pattern recognition receptors (PRRs) [7–9]. Signal transduction depends on the expression of a family of type I transmembrane receptors, Toll-like receptors (TLRs). To date, 11 TLRs have been identified in humans; they are expressed primarily on cell types that are mammalian host immune-competent cells such as dendritic cells and macrophages. These are the cells that are most likely to come into direct contact, via the mucosal epithelia, with pathogens from the environment [10]. TLR expression is not restricted to phagocytic cell types, rather, it appears that the majority of cells in the body including mucosal epithelial cells express at least a subset of TLRs [11]. Some PRRs are located on the cell membrane and respond to extracellular PAMPs; others exist in the cytosol and respond to PAMPs that cross the plasma membrane [12–14]. Signaling through TLRs results in the activation of IKK, NF-κB, and NF-κB target genes, and the coordinated activation of several transcription factors that regulate the expression of antimicrobial genes, cytokines, chemokines, and co-stimulatory molecules [7–9].

* Corresponding author. Fax: +81 75 251 5663.
E-mail address: mueta@ophth.kpu-m.ac.jp (M. Ueta).

0006-291X/$ - see front matter © 2005 Elsevier Inc. All rights reserved.
doi:10.1016/j.bbrc.2005.02.196

Although the eye is relatively impermeable to microorganisms [1,3,15,16], if corneal integrity is compromised by trauma or contact lens wear, sight-threatening bacterial infection may occur [17,18]. Uniquely, human corneal epithelial cells (HCEC) are in constant contact with bacteria and bacterial products; they form a structural and functional barrier against numerous bacteria both pathogenic and nonpathogenic. Factors normally pro-inflammatory for other cell types do not induce epithelial cells to initiate a defensive response [19]. This is especially important with respect to the epithelial cells of the avascular and transparent cornea, where the formation of scar tissue in response to a host inflammatory reaction results in opacification and loss of vision. We previously reported that human corneal epithelial cells failed to respond functionally to PAMPs such as peptidoglycan (PGN) and lipopolysaccharide (LPS) because they lack TLR2 and TLR4 on their surface [20]. Despite the existence of TLR2 and TLR4 in the cytoplasm of HCEC, the experimental translocation of LPS to the cytoplasm did not elicit an immune response [20].

Among the TLRs, TLR4 which recognizes LPS, and TLR3 which recognizes the viral double-stranded RNA-mimic polyI:C have received the greatest attention [21–23]. TLR3-mediated responses are unique because TLR3 activation elicits lower levels of inflammatory cytokines than the activation of other TLR family members, although TLR3 activation induces the very robust secretion of IFN-β [21]. The remarkable similarities in the cellular responses to bacterial and viral infection after pathogen recognition are indicative of cross-talk between virus- and bacteria-induced signaling [24]. Although there were two reports by the same group describing the inhibitory effect of polyI:C against herpetic keratitis in rabbits, nothing is yet known on the reproducibility of their experiments or the effect on the innate immune response [25,26].

Here we demonstrate that HCEC express TLR3 at the cell surface and thus respond to polyI:C to generate pro-inflammatory cytokines and IFN-β. We also show that the surface expression of TLR3 on HCEC was amplified in an autocrine/paracrine manner by polyI:C.

Materials and methods

All experimental procedures were conducted in accordance with the principles set forth in the Helsinki Declaration. The purpose of the research and the experimental protocols were explained to all participants and their prior written informed consent was obtained.

Human corneal epithelial cells. For RT-PCR, human corneal epithelial cells (HCEC) were obtained from corneal buttons of patients undergoing corneal transplantation for early-stage bullous keratopathy (one eye) or keratoconus (two eyes) at the affiliated hospital of Kyoto Prefectural University of Medicine.

Primary HCEC, obtained from Kurabo (Osaka, Japan), were cultured at 37 °C under 95% humidity and 5% CO_2 in serum-free medium consisting of EpiLife (Kurabo) supplemented with HCEC growth supplement (HCGS) containing 1 ng/ml murine epidermal growth factor (mEGF), 5 μg/ml insulin from bovine pancreas, 0.18 μg/ml hydrocortisone, and 0.4% v/v bovine pituitary extract (Kurabo), 0.2% PSA solution, and antibiotic–antimycotic solution (5000 U/ml penicillin, 50 mg/ml streptomycin, and 12.5 μg/ml amphotericin B) (Kurabo) [20]. For assays, 2×10^6 primary HCEC were plated in 25 cm^2 flasks. After reaching sub-confluence, they were either left untreated, exposed to 1 μg/ml LPS from *Pseudomonas aeruginosa* (Sigma, St. Louis, MO), or exposed to 25 μg/ml polyI:C (Invivogen, San Diego, CA) for 1-, 3- or 6 h. The culture time of polyI:C-treated cells was adjusted to be optimal for the maximum induction of IL-6, IFN-β, IκBα, MAIL, and TLR3, it was 6 h for IL-6, IL-8, and TLR3, and 3 h for IFN-β, IκBα, and MAIL.

Purification of human peripheral mononuclear cells. Venous blood samples from healthy volunteers were anti-coagulated with 2Na-EDTA, placed in sterile 50-ml polypropylene tubes, mixed with 1 volume of Ca^{2+}-free PBS (PBS(−)), overlaid with Ficoll–Paque Plus (Amersham Biosciences AB, Uppsala, Sweden), and centrifuged for 20 min at 2000 rpm at 20 °C. Human peripheral mononuclear cells (HPMC) were gently aspirated from the interface and washed with PBS(−). For stimulation with LPS or polyI:C, isolated HPMC were cultured for 1-, 3- or 6 h in RPMI medium (Gibco-BRL Life Technologies, Paisley, UK) supplemented with 10% fetal calf serum (Gibco) and 1% antibiotic–antimycotic solution (100 U/ml penicillin, 100 mg/ml streptomycin, and 250 ng/ml amphotericin B) (Gibco).

Human conjunctival fibroblasts. Human conjunctival fibroblasts (HCFB) were obtained from redundant subconjunctival tissues of patients undergoing cataract surgery at the affiliated hospital of Kyoto Prefectural University of Medicine. Primary HCFB were cultured in DMEM (Gibco) supplemented with 10% fetal calf serum (Gibco) and 1% antibiotic–antimycotic solution (100 U/ml penicillin, 100 mg/ml streptomycin, and 250 ng/ml amphotericin B) (Gibco). For assays, all procedures were the same as those described above for HCEC.

MRC-5 and HeLa cells. MRC-5 and HeLa, expressing TLR3 on the cell surface and producing IFN-β upon polyI:C stimulation, were the gift of Dr. T. Seya (Hokkaido University). MRC-5, normal human lung fibroblasts, and HeLa cells were maintained in MEM (Gibco) supplemented with 1% antibiotic–antimycotic solution (100 U/ml penicillin, 100 mg/ml streptomycin, and 250 ng/ml amphotericin B) (Gibco), and 10% or 5% fetal calf serum (Gibco). For assays, all procedures were the same as those described above for HCEC.

RT-PCR. Total RNA was isolated from human corneal epithelium and HPMC using Trizol Reagent (Life Technologies, New York, NY) according to the manufacturer's instructions. For the RT reaction, we used the SuperScript Preamplification kit (Invitrogen). PCR amplification was performed with DNA polymerase (Takara; Shiga, Japan) for 38 cycles at 94 °C for 1 min, annealing for 1 min, and 72 °C for 1 min on a commercial PCR machine (GeneAmp; PE Applied Biosystems). The primers we used are listed in Table 1. The integrity of the RNA was assessed by electrophoresis in ethidium bromide-stained 1.5% agarose gels.

Flow cytometric analysis. Human primary corneal epithelial cells were treated with 0.02% EDTA. The cell-surface expression of TLR2, TLR3, and TLR4 was examined by flow cytometry. For TLR3 expression, cells were incubated with mouse anti-human TLR3 monoclonal antibody (mAb; Imgenex, San Diego, CA) or isotype control mouse IgG1 (DakoCytomation, Kyoto, Japan) for 30 min at 4 °C. Alexa Fluor 488 goat anti-mouse IgG (H + L) (Molecular Probes, Eugene, OR) was used as the secondary antibody. For TLR2 and TLR4 expression, cells were incubated for 30 min at 4 °C with PE-conjugated mouse anti-human TLR2 (TL2.1), TLR4 (HTA125) monoclonal antibody (eBioscience, San Diego, CA), or isotype control mouse IgG2a (BD PharMingen). Stained cells were analyzed with a FACSCalibur (Becton–Dickinson, San Jose, CA); data were analyzed using Cellquest software (Becton–Dickinson). Moreover, HCFB, MRC-5, and HeLa were examined for their cell-surface expression of TLR3.

Table 1
The primer list of TLRs

Gene	Accession No.		Primers	Bases	Product size (bp)	Annealing
TLR1	NM003263	Sense	5′-TGCCCTGCCTATATGCAA-3′	(381–398)	555	54
		Anti-sense	5′-GAACACATCGCTGACAACT-3′	(918-936)		
TLR2	XM003304	Sense	5′-GCCAAAGTCTTGATTGATTGG-3′	(1783–1803)	346	52
		Anti-sense	5′-TTGAAGTTCTCCAGCTCCTG-3′	(2110–2129)		
TLR3	NM003265	Sense	5′-CGCCAACTTCACAAGGTA-3′	(277–294)	689	54
		Anti-sense	5′-GGAAGCCAAGCAAAGGAA-3′	(949–966)		
TLR4	XM005336	Sense	5′-TGGATACGTTTCCTTATAAG-3′	(1768–1787)	506	52
		Anti-sense	5′-GAAATGGAGGCACCCCTTC-3′	(2256–2274)		
TLR5	NM003268	Sense	5′-ATCTGACTGCATTAAGGGGAC-3′	(2274–2294)	567	52
		Anti-sense	5′-TTGAGCAAAGCATTCTGCAC-3′	(2822–2841)		
TLR6	NM006068	Sense	5′-CCTCAACCACATAGAAACGAC-3′	(832–852)	531	50
		Anti-sense	5′-CACCACTATACTCTCAACCCAA-3′	(1342–1363)		
TLR7	NM016562	Sense	5′-AGTGTCTAAAGAACCTGG-3′	(2222–2239)	544	50
		Anti-sense	5′-CCTGGCCTTACAGAAATG-3′	(2749–2766)		
TLR8	NM016610	Sense	5′-CAGAATAGCAGGCGTAACACATCA-3′	(1909–1932)	639	56
		Anti-sense	5′-AATGTCACAGGTGCATTCAAAGGG-3′	(2522–2545)		
TLR9	NM017442	Sense	5′-GTGCCCCACTTCTCCATG-3′	(791–808)	259	50
		Anti-sense	5′-GGCACAGTCATGATGTTGTTG-3′	(1030–1050)		
TLR10	NM030956	Sense	5′-CTTTGATCTGCCCTGGTATCTC-3′	(2286–2307)	497	52
		Anti-sense	5′-AGCCCACATTTACGCCTATCCT-3′	(2783–2286)		
GAPDH	XM033263	Sense	5′-CCATCACCATCTTCCAGGAG-3′	(293–312)	575	60
		Anti-sense	5′-CCTGCTTCACCACCTTCTTG-3′	(849–868)		

ELISA. To quantify cytokine secretion, culture supernatants were harvested and the level of IL-6 and IL-8 was assayed by human cytokine-specific ELISA (Biosource, Camarillo, CA).

Real-time semi-quantitative PCR. This was performed on an ABI-prism 7700 (Applied Biosystems, Foster City, CA) according to a previously described protocol [27] and the manufacturer's instructions. Total cellular RNA extraction and the first cDNA synthesis were as described above. The primers and probes for human IFN-β, human molecules possessing ankyrin-repeats induced by LPS (MAIL), and human GAPDH were from Perkin-Elmer Applied Biosystems. Previously reported primer and TaqMan probes for human IL-6 and IL-8 were used. The primers for IL-6 were 5′-TGACAAACAAATT CGGTACATCCT-3′ and 5′-AGTGCCTCTTTGCTGCTTTCAC-3′; the TaqMan probe for human IL-6 was 5′-TTACTCTTGTTACA TGTCTCCTTTCTCAGGGCTG-3′ [28]. The primers for human IL-8 were 5′-GCGCCAACACAGAAATTATTGTAA-3′ and 5′-TTATGA ATTCTCAGCCCTCTTCAA-3′; the TaqMan probe for IL-8 was 5′-TTCTCCACAACCCTCTGCACCCAGTT-3′ [27]. The probes were synthesized by Perkin-Elmer Applied Biosystems. To amplify human IL-6, IL-8, IFN-β, MAIL, and GAPDH cDNA, PCR was performed in a 25-μl total volume that contained a 1 μl cDNA template in 2× TaqMan universal PCR master mix (Applied Biosystems) at 50 °C for 2 min and 95 °C for 10 min, followed by 40 cycles at 95 °C for 15 s and 60 °C for 1 min. The results were analyzed with sequence detection software (Applied Biosystems); the expression level of each mRNA was normalized to the expression of the human housekeeping gene GAPDH.

Data analysis. Data were expressed as means ± SE and evaluated by Student's *t* test using the Excel program.

Results

Expression of TLR3-specific mRNA in human corneal epithelium

We first examined whether human corneal epithelium expresses specific mRNA for TLRs 1–10. TLR-specific RT-PCR showed that mRNA from all but TLR8 was present in normal human corneal epithelium (Fig. 1). Among TLR-specific mRNA tested, TLR3 was expressed most intensely. When, as a positive control, we also subjected mRNA isolated from HPMC to RT-PCR, we found that these cells expressed TLRs 1–10. We then isolated, subcloned, and sequenced the PCR products. The obtained sequences were >95% identical with the known nucleotide sequences of human TLRs. Our findings suggest that while human corneal epithelium harbors messages for most TLRs, TLR3 is the one with the highest expression level. The expression of TLR3 was higher, while that of the other TLRs was lower, in human corneal epithelium than HPMC.

Primary HCEC express TLR3, but not TLR2 and TLR4, on the cell surface

Next we examined the cell-surface expression of TLR2, TLR3, and TLR4 on primary HCEC. While TLR3 was expressed on the surface of primary HCEC, TLR2 and TLR4 were not (Fig. 2). In positive controls, TLR2 and TLR4 were expressed on the cell surface of human peripheral blood monocytes and TLR3 was expressed on the cell surface of MRC-5 [29].

Primary HCEC respond to polyI:C but not LPS

Next we determined whether HCEC respond to polyI:C, a mimic of TLR3 ligand dsRNA. We first examined the production of inflammatory cytokines by primary HCEC stimulated with polyI:C and LPS. As

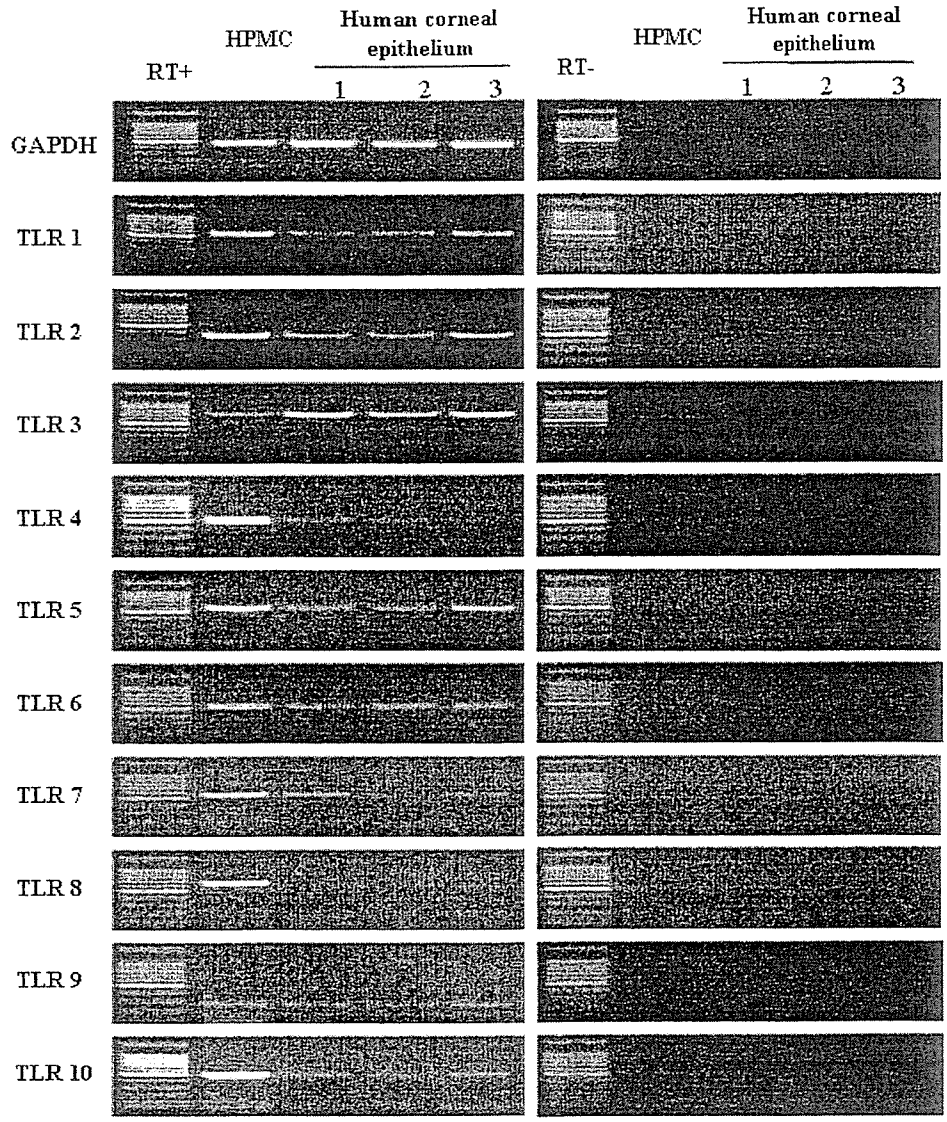

Fig. 1. The level of TLR3 expression is higher in human corneal epithelium than HPMC. Normal human corneal epithelium expresses mRNAs for TLRs 1–7 and 9–10 but not TLR8. As a positive control, mRNA isolated from human peripheral mononuclear cells (HPMC) was subjected to RT-PCR (left column). RT– indicates data were obtained without reverse transcription (controls).

shown in Fig. 3A, polyI:C stimulation induced the secretion of IL-6 and IL-8 while LPS treatment did not; in LPS-treated primary HCEC the level of IL-6 and IL-8 was similar to that seen in unstimulated cells. On the other hand, LPS stimulation significantly increased the production of IL-6 and IL-8 by HPMC and HCFB.

These findings were confirmed at the mRNA expression level. In primary HCEC, stimulation with polyI:C, but not LPS, resulted in the increased expression of IL-6- and IL-8-specific mRNA. Conversely, HPMC responded to LPS- but not to polyI:C stimulation and HCFB responded to both LPS and polyI:C (Fig. 3B).

IFN-β is controlled with TLR3/IRF-3 signaling. Thus, IFN-β-specific mRNA was significantly elevated in polyI:C- but not LPS-stimulated primary HCEC. Similarly, polyI:C but not LPS stimulated the induction of IFN-β in HPMC and HCFB. Surprisingly, IFN-β-specific mRNA expression was markedly higher in primary HCEC than HPMC and HCFB (Figs. 4A and B). Although primary human fibroblasts such as HCFB and MRC-5 expressed TLR3 on their cell surface, the cell-surface expression of TLR3 was more notable in primary HCEC (Fig. 4C).

Induction of IκBα- and MAIL-specific mRNA by polyI:C, but not LPS, in primary HCEC

In epithelial cells, the transcription factor NF-κB plays a central role in regulating genes that govern the onset of mucosal inflammatory responses. The primary consequences of TLR activation are NF-κB activation, cytokine secretion, and the expression of co-stimulatory molecules [9,30]. These responses help to promote and shape the critical immunological processes that facilitate

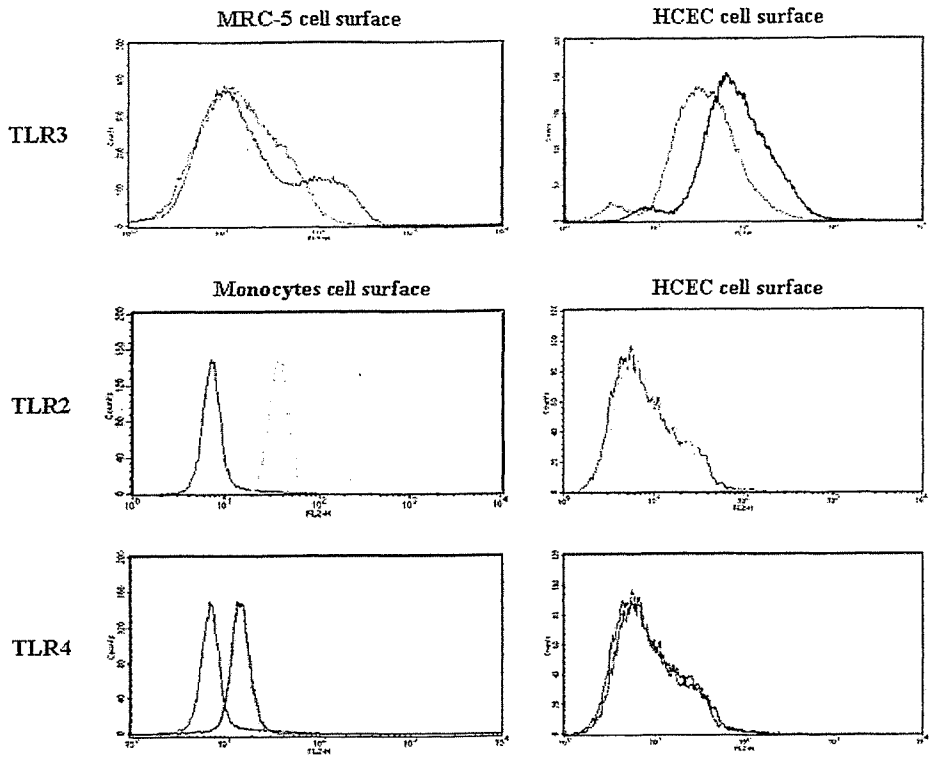

Fig. 2. Primary HCEC express TLR3, but not TLR2 and TLR4, on the cell surface. The cell-surface expression of TLR2, TLR3, and TLR4 was examined by flow cytometry. For TLR3 expression, cells were incubated (30 min, 4 °C) with mouse anti-human TLR3 monoclonal antibody or isotype control mouse IgG1. Alexa Fluor 488 goat anti-mouse IgG (H + L) was the secondary antibody. For TLR2 and TLR4 expression, cells were incubated (30 min, 4 °C) with PE-conjugated mouse anti-human TLR2 (TL2.1), TLR4 (HTA125) monoclonal antibody, or isotype control mouse IgG2a. The histogram data are representative of three separate experiments.

the control and clearance of pathogens. We examined whether polyI:C stimulation of primary HCEC induced mRNA specific for the IκB family, regulators of NF-κB, such as IκBα and MAIL. We found that the expression of IκBα- and MAIL-specific mRNA was in fact elevated by polyI:C but not LPS (Fig. 5). These mRNAs were not up-regulated in polyI:C-stimulated HPMC, but their expression was significantly up-regulated upon stimulation with LPS as described previously [31]. It is of note that MAIL-specific mRNA was elevated by both polyI:C and LPS in HCFB. Taken together, these findings show that polyI:C could up-regulate IκBα and MAIL expression in primary HCEC via TLR3 (Fig. 5).

PolyI:C stimulates the gene expression and surface expression of TLR3 in primary HCEC

In macrophages, high TLR3- but not TLR4 gene expression levels are induced by TLR3 and TLR4 agonists [32]. In the context of this autocrine loop of TLR3 expression, we examined whether TLR-specific mRNA was inducible in primary HCEC by the TLR3 agonist polyI:C. As shown in Fig. 6A, TLR3-specific mRNA was highly elevated in primary HCEC stimulated with polyI:C. Interestingly, increased TLR2 and TLR4 gene expression was also observed in polyI:C- but not LPS-stimulated primary HCEC. Furthermore, as shown in Fig. 6B, the cell-surface expression of TLR3, but not of TLR2 and TLR4, was increased. These observations raise interesting questions regarding the role of TLR3 in the host defense mounted by corneal epithelium.

Discussion

We provide evidence for the gene and surface expression of TLR3 in human corneal epithelium and suggest that expressed TLR3 is functionally active in the secretion of the inflammatory mediators IL-6, IL-8, and IFN-β. We thus documented that polyI:C can induce the secretion of inflammatory mediators by primary HCEC. The ability of IFN-β to prevent the death of anergic cells, in addition to its anti-proliferative effect, may be one way in which the immune system regains a quiescent state after activation [33]. Further studies are necessary to elucidate the pathological role of IFN-β produced by HCEC. It is noteworthy that TLR3 expression was up-regulated by the TLR3 agonist polyI:C. Furthermore, the up-regulation in primary HCEC of IκB-α and MAIL (a human homologue of IκBζ, a NF-κB regulator in the nucleus) by polyI:C suggests a

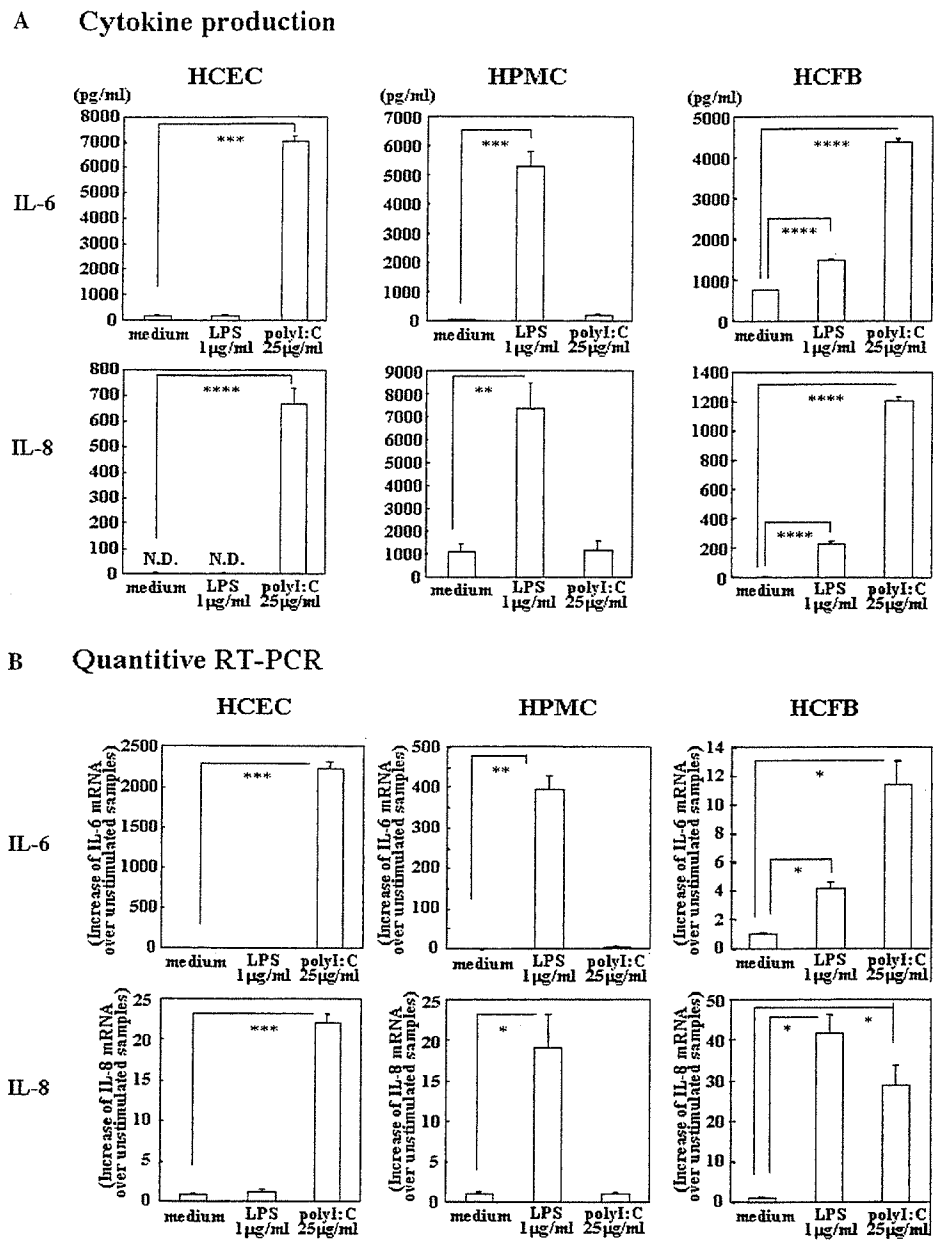

Fig. 3. The production and mRNA expression of IL-6 and IL-8 by primary HCEC. Primary HCEC and HCFB were cultured to sub-confluence and exposed to 1 μg/ml LPS from *P. aeruginosa* or 25 μg/ml polyI:C for 6 h. HPMC were cultured at a density of about 1×10^6 cells/ml and exposed to either 1 μg/ml LPS from *P. aeruginosa* or 25 μg/ml polyI:C for 6 h. (A) The culture supernatants were harvested and assayed by cytokine-specific ELISA for IL-6 and IL-8. (B) Total RNA was isolated from these cells with the Trizol reagent (Life Technologies). The RT reaction was performed with the SuperScript preamplification system (Invitrogen). Real-time semi-quantitative PCR was on an ABI-prism 7700. The *Y* axis shows the increase of specific mRNA over unstimulated samples. Data are representative of three separate experiments and show means ± SEM from an experiment carried out in triplicate wells (*$p < 0.05$; **$p < 0.01$; ***$p < 0.005$; and ****$p < 0.001$).

novel role for TLRs in ocular surface physiology. The new findings presented here contribute to a better understanding of innate ocular surface immunity.

A novel IκB protein, IκBζ/MAIL, induced by IL-1 and PAMPs regulates NF-κB in the cell nucleus. The induction of IκBζ is controlled by NF-κB, which, in turn, is negatively regulated by IκBζ, thereby forming an autonomous negative-feedback loop [34]. We postulate that IκBζ in ocular surface epithelium negatively regulates the pathological progression of ocular surface inflammation [35].

IκBζ was originally reported as a regulator of NF-κB induced by IL-1 and LPS [36]. LPS stimulation induced IκBζ in macrophages [31,34], but not primary HCEC (Fig. 4C). Furthermore, IκBζ is reportedly indispensable for IL-6 production in response to TLR ligands and is a positive regulator of NF-κB in the two-step process of IL-6 gene activation [37]. The implications of the

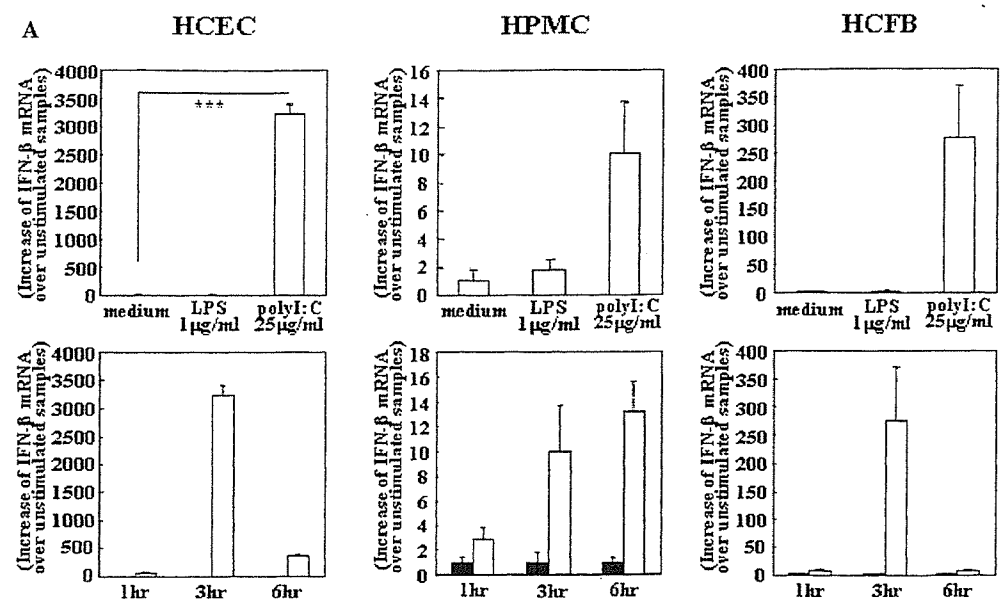

B The ratio of IFN-β/GAPDH mRNA at 3hr

	HCEC	ratio to HCEC	HPMC	ratio to HCEC	HCFB	ratio to HCEC	MRC-5	ratio to HCEC	HeLa	ratio to HCEC
unstimulated samples	0.00074 ±0.00014	1	0.01821 ±0.01295	24.6	0.00031 ±0.00002	4/10	0.00003 ±0.00002	4/100	0.0004 ±0.00013	5/10
stimulated with polyI:C	2.39136 ±0.13371	1	0.14682 ±0.06039	6/100	0.11038 ±0.01085	5/100	0.0462 ±0.00201	2/100	0.0468 ±0.00338	2/100
increasing ratio	3224	1	8	2/1000	360	1/10	1540	5/10	117	4/100

C Cell surface expression of TLR3

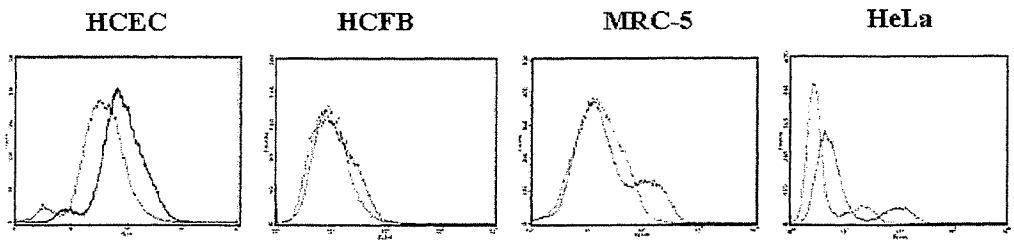

Fig. 4. Comparison of IFN-β mRNA expression and TLR3 cell-surface expression. (A) HCEC, HCFB, and HPMC were cultured as in Fig. 3 and exposed to either 1 μg/ml LPS from *P. aeruginosa* or 25 μg/ml polyI:C for 3 h. Subsequent procedures were as in the assay of mRNA expression. The *Y* axis shows the increase of specific mRNA over unstimulated samples. Data are representative of two separate experiments and show means ± SEM from an experiment carried out in triplicate wells (***$p < 0.005$). (B) The methods were as in (A). The actual ratio of IFN-β/GAPDH mRNA and the relative ratio in HCEC are summarized in the table. (C) Cell-surface expression of TLR3 was examined by flow cytometry. Cells were incubated (30 min, 4 °C) with mouse anti-human TLR3 monoclonal antibody or isotype control mouse IgG1. Alexa Fluor 488 goat anti-mouse IgG (H + L) was the secondary antibody. The histogram data are representative of three separate experiments.

induction by polyI:C of IκBζ/MAIL in primary HCEC remain to be determined.

The epithelial expression of TLRs may be of importance in inflammation and immunity in response to pathogens [38–41]. Unique patterns of TLR expression appear to exist at different host-environment tissue interfaces. Under physiological conditions, the corneal epithelium appears to be hyporesponsive to commensal bacteria to which it is consistently exposed. We previously reported that HCEC failed to respond functionally to LPS or PGN because they lack TLR2 and TLR4 on their cell surface [20]. Despite the presence of TLR2 and TLR4 in their cytoplasm, HCEC did not respond to experimentally translocated LPS [20]. This is indicative of a characteristic difference between HCEC and immune-competent cells such as macrophages. The selective expression of TLR3 in human corneal epithelium (Fig. 1) contrasts with the ubiquitous expression of TLR family members in HPMC and indicates that the regulation and localization of TLR3 are different

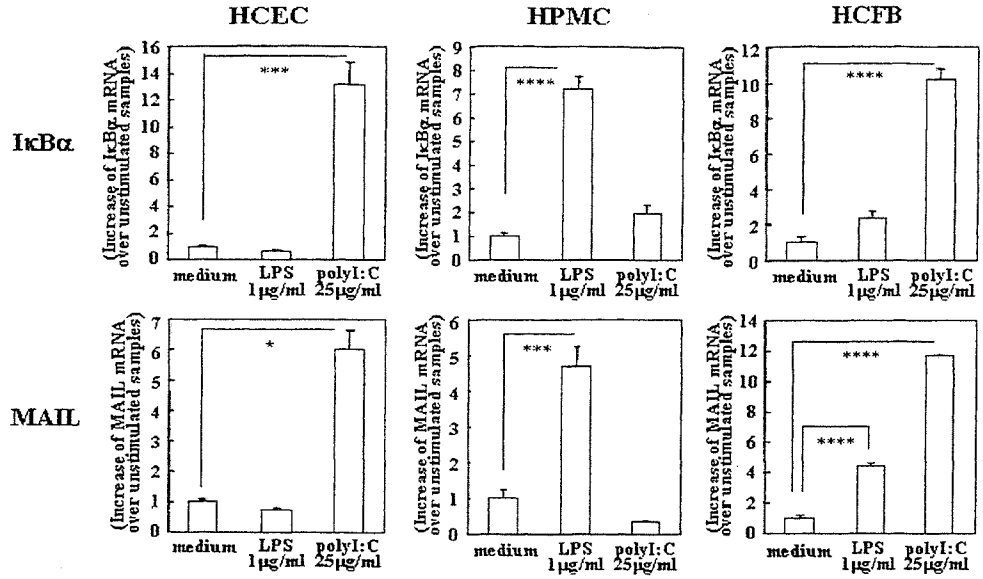

Fig. 5. Augmentation of MAIL and IκB-α gene expression in polyI:C-stimulated primary HCEC. HCEC, HCFB, and HPMC were cultured as in Fig. 3 and exposed to either 1 μg/ml LPS from *P. aeruginosa* or 25 μg/ml polyI:C for 3 h, subsequent procedures were as in the assay of mRNA expression. The *Y* axis shows the increase of specific mRNA over unstimulated samples. Data are representative of two separate experiments and show means ± SEM from an experiment carried out in triplicate wells (*$p < 0.05$; ***$p < 0.005$; and ****$p < 0.001$).

in these cells. This may reflect the participation of cell type-specific multiple pathways in antiviral IFN induction via TLR3 [42]. However, the previous work does not exclude the role of inflammation-dependent TLRs on HCEC or on antigen-presenting cells infiltrating corneal tissue. IFN-α up-regulated TLR3 mRNA expression in epithelial cells and IFN-γ enhanced TLR3 expression in epithelial- and endothelial cells [43]. In macrophages, TLR3 expression is inducible by both TLR3 and TLR4 ligands, although these stimuli fail to induce TLR4 expression. Furthermore, TLR3 and TLR4 require the IFN-β autocrine/paracrine feedback mechanism to induce TLR3 expression and to activate and/or enhance genes required for antiviral activity [32]. IFN-α/β is critical for the measles virus-mediated up-regulation of TLR3 induction [44]. Given that cell-surface TLR3 expression was up-regulated by an agonist of TLR3, polyI:C (Fig. 6), and that polyI:C was able to induce the gene expression of IFN-β in HCEC (Fig. 4B), it is conceivable that IFN-β is crucial for the innate immune response of the ocular surface to pathogenic and nonpathogenic viruses and bacteria.

LPS up-regulates TLR3 expression in murine phagocytic cells through autocrine IFN-β induction. In humans, however, the IFN-β-induced up-regulation of TLR3 was blocked by pretreatment with LPS [45]. This observation coincides with our present results that TLR3 expression was not up-regulated by an agonist of TLR4, LPS (Fig. 6), and that LPS was incapable of inducing the gene expression of IFN-β in HCEC (Fig. 4A). The species-specific differences between humans and mice in their responses to LPS coincide with the presence of different, evolutionary nonconserved promoter sequences in both species. The intriguing functionality of TLR3 in HCEC and the far more potent induction of IFN-β by a TLR3 agonist in HCEC than fibroblasts require elucidation of the molecular mechanisms that regulate TLR3 expression on HCEC.

Although all TLRs activate NF-κB, not all TLRs activate IRF3 or induce IFN-β expression. TLR3 and TLR4 are the best-characterized TLRs known to activate IRF3 [30]. The TIR domain-containing adapter-inducing IFN-β (TRIF) is also an adapter for TLR3 and TLR4 [46,47]. Unlike the other TLRs including TLR4 that use the common MyD88-dependent pathway, TLR3 seems to employ only MyD88-independent TRIF-dependent pathways. These biochemical findings may account for the distinctly different responses elicited by polyI:C and LPS in the present study.

Type I IFN is induced not only by viral but also by bacterial infection [22,48]. An understanding of the role of the TLR3-IFN-β-link is crucial for understanding the involvement of type I IFN in TLR3-induced biological effects on the ocular surface. O'Conell et al. [49] reported that type I IFNs play a different role in bacterial and viral infections. The sophisticated interplay between bacteria and viruses may culminate in the exacerbation of pathological inflammation on the ocular surface.

In summary, the innate immune responses in mucosal epithelial cells such as HCEC differ from those in immune-competent cells such as macrophages. The elucidation of the unique innate immune response in mucosal epithelium is critical for a better understanding of the symbiotic relationship between mucosal epithelial cells and commensal bacteria inhabiting the mucosal surface.

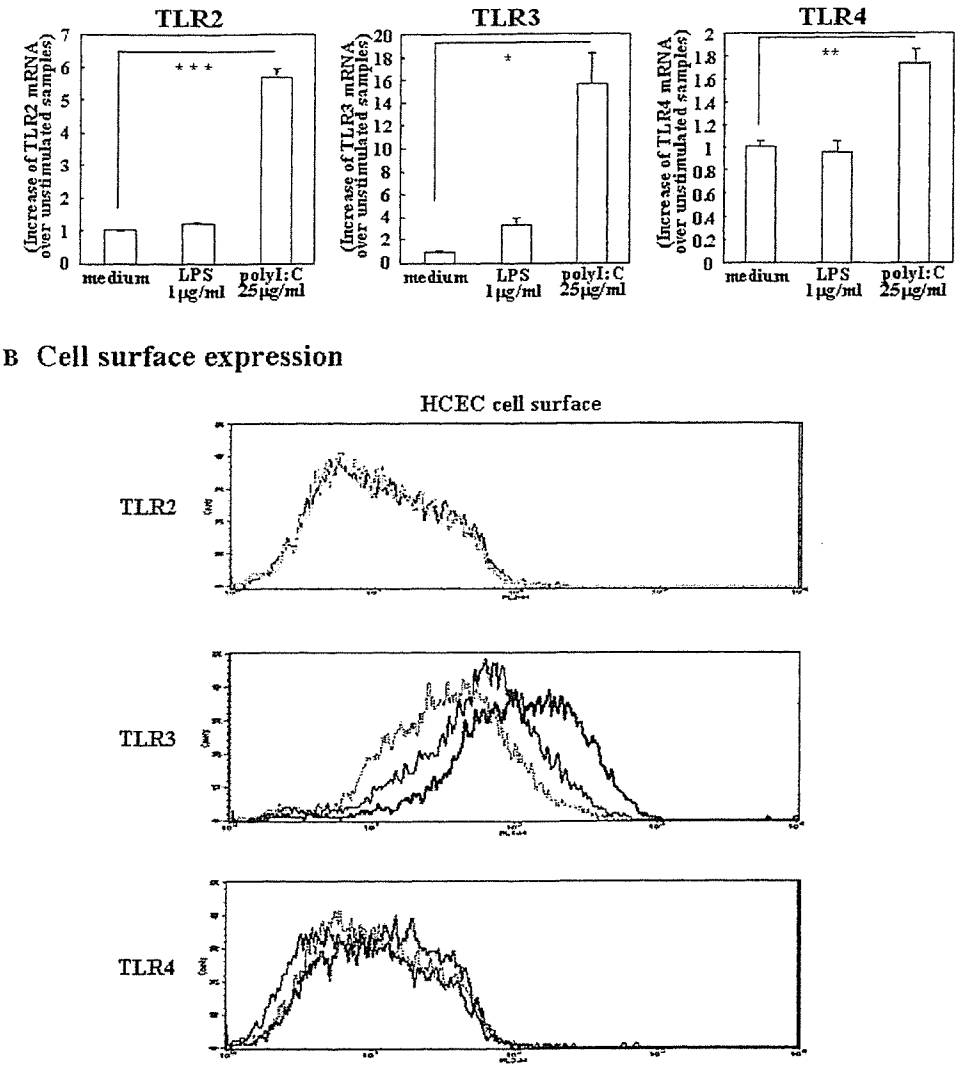

Fig. 6. Augmentation of TLR3 expression on HECE by polyI:C stimulation. (A) Augmentation of TLR3 gene expression in polyI:C-stimulated primary HCEC. Primary HCEC were cultured to sub-confluence in 25 cm^2 flasks (2×10^6 cells/flask) and exposed to 1 μg/ml LPS from *P. aeruginosa* or 25 μg/ml polyI:C for 6 h. RNA extraction, RT reaction, and real-time semi-quantitative PCR were as in Fig. 3. The *Y* axis shows the increase of specific mRNA over unstimulated samples. Data are representative of three separate experiments and show means ± SEM from an experiment carried out in triplicate wells. (B) Augmentation of TLR3 cell-surface expression on polyI:C-stimulated primary HCEC. Primary HCEC were cultured to sub-confluence in 75 cm^2 flasks (6×10^6 cells/flask) and untreated or exposed to 25 μg/ml polyI:C for 6 h. The cell-surface expression of TLR2, TLR3, and TLR4 was examined by flow cytometry. For TLR3 expression, cells were incubated (30 min, 4 °C) with mouse anti-human TLR3 monoclonal antibody or isotype control mouse IgG1. Alexa Fluor 488 goat anti-mouse IgG (H + L) was the secondary antibody. For TLR2 and TLR4 expression, cells were incubated (30 min, 4 °C) with PE-conjugated mouse anti-human TLR2 (TL2.1), TLR4 (HTA125) monoclonal antibody, or isotype control mouse IgG2a. The histogram data are representative of two separate experiments (dotted line, isotype control; thin line, untreated; and bold line, stimulated with 25 μg/ml polyI:C for 6 h).

Acknowledgments

This work was supported in part by Grants-in-Aid for scientific research from the Japanese Ministry of Health, Labour and Welfare, the Japanese Ministry of Education, Culture, Sports, Science and Technology, CREST from JST, a research grant from the Kyoto Foundation for the Promotion of Medical Science, and the Intramural Research Fund of Kyoto Prefectural University of Medicine. We thank Dr. T. Seya and Dr. J. Yamada for the gift of MRC5, HeLa cells, and HCFB, respectively, and Ms. C. Mochida for her technical assistance.

References

[1] R.J. Haynes, P.J. Tighe, H.S. Dua, Br. J. Ophthalmol. 83 (1999) 737–741.
[2] J.W. Streilein, Nat. Rev. Immunol. 3 (2003) 879–889.